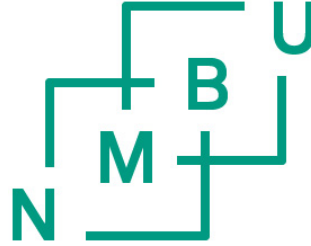NORWEGIAN UNIVERSITY OF LIFE SCIENCES

MASTER THESIS

Collaps capacity for a pipeline with thick coating

| *Author:* | *Supervisor:* | *Co-supervisor:* |
| Ramin Lam JAMEDARI | Odd-Ivar LEKANG | Olav AAMLID |

A thesis submitted in fulfilment of the requirements
for the degree of Master of Science

in the

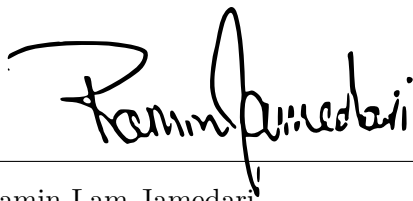Department of Mathematical Sciences and Technology

May 2015

Preface

This report is the result of my Master's Thesis work done in the spring semester 2015 at the Department of Mathematical Sciences and Technology- IMT at the Norwegian University of Life Sciences. The project has been caried out at, and in collabration with Den Norske Veritas, DNV-GL in Høvik, Bærum.

The deepwater oil and gas reservoars are becomming increasingly important to the global hydrocarbon supply. When a pipe is laid at large depths is required that the wall thickness is sufficient to withstand the outer pressure. Existing design formulas for collapse are neglecting the effect of pipeline coating. It has been therefore of great interest to the industry to investigate if todays practice of neglecting the coating is acceptable.

I would like to express my special thanks to DNV-GL and co-supervisor Dr. Olav Aamlid for trusting with this task and giving me the opportunity to be a part of the *Pipeline and Operations Technology* department for the duration of this project. My sincerest thanks to all individuals at DNV-GL for showing their interest in the project and helping me out with technical questions from time to time. Also thanks to my supervisor Odd-Ivar Lekang for his advise throughout the project.

Finally a special gratitude to my wife for her support and patience, also to my daughter in keeping me awake at night. This would be simply very much harder without them.

Ramin Lam Jamedari	11.05.2015
	Dato

Abstract

When a pipeline is installed at deep waters the primary design load is the external pressure, hence making the collapse pressure the major design parameter. Pipeline collapse formulas are functions of elastic and plastic collaspe pressure acompanied the initial ovality and yield stress. The most common formulas for collapse are the *Timoshenko*, *Shell* and *Haagsma* equation where the latter is the least conservative and used in the offshore standard DNV-OS-F101.

In any pipeline system onshore or offshore there is a need of pipeline protection. The purpose of coating is to isolate the pipeline steel from the seawater, the soil and to introduce a high resistance path between anodic and cathodic areas. Such coatings can be ranging from a few up to around hundred millimeter, thus the cros section of the coated pipe can be many times initial cros section of the bare steel pipe.

Existing design formulas for collapse are neglecting the effect of pipeline coating and a study is proposed to investigate if todays practice of neglecting the coating is acceptable.

In this project ABAQUS finite element software has been used to examine a coated pipe section with various thicknesses, elasticity and ovality and compared the collapse limit to the values of a uncoated pipe.

Based on the assumption of elasticity and material model of coating the results has shown to increase the collapse capacity when the coating thickness and elasticity increases. The values has shown a increase in range of 5 to 25 %. The ovality of the coating however has shown to not effect the pipe collapse capacity in any significant way.

Also based on a proposed simple analytical collapse model of serial resistance where the collapse capacity of the steel pipe is added to the collapse capacity of the coated pipe without the steel, the model has shown a good agreement with ABAQUS collapse data and thus is recommended for use in collapse calculation of coated pipelines.

For future work a study is proposed to investigate the possibilities of steel pipe wall thickness reduction when adding thick coating to a line pipe

Sammendrag

Når undersjøiske rørledninger blir innstallert ved dypt vann vil den primære og største lastfaktoren være det ytre overtrykket. Utfordringen vil da som følge av dette være å ungå rørsvikt ved kollaps. Dagens kollapskapasitetsmodeller er basert på samspillet mellom elastisk og plastisk kollaps kapasitet, samt rørets ovalitet. De mest kjente modelene er *Timoshenko*, *Shell* og *Haagsma* ligningen, hvorav den siste nevnte er den minst konservative og blir brukt i DNV-GL sitt rør standard DNV-OS-F101.

For enhver rørsystem både offshore og onshore vil det alltid være behov for rør beskyttelse i form av belegg. Hensikten med belegg er å beskytte røret mot saltvann, friksjon krefter fra havbunnen, samt introdusere et hinne mellom det anodiske og det katodiske miljøet. Slikt belegg kan variere i tykkelse fra noen få til mer enn 100 milimeter. Således kan tvernitts arealet til et rør med belegg ha flere ganger arealet av det ubeskyttede stålrøret.

Dagens formelverk for kollaps av rør neglisjerer effekten av et slikt belegg og derfor har dette prosjektet blitt dedikert til å undersøke om hvorvidt denne praksisen er innenfor grensene av sikker design.

I dette prosjektet har ABAQUS programvare blitt brukt til element analyse av et rør stykke hvor rørets belegg har variert i tykkelse, elastisitet og ovalitet. Kollaps data har således blitt sammenlignet med et rør uten belegg.

Basert på den antatte materiale modellen for belegget har analysen påvist en positiv endring i kollaps kapasitet når beleggets tykkelse, elastisitet og da stivhet har økt. Økningen av resistansen ble påvist til mellom 5 og 25 %. Samtidig har analysen ikke påvist noen signifikante endringer som følge av beleggets ovalitet.

Denne oppgaven har introdusert en enkel analytisk model for beregning av kollaps av rør med belegg. Denne modellen har vist seg å stemme godt overens med ABAQUS kollaps data og blir anbefalt brukt ved fremtidige beregninger.

For fremtidig arbeid er et studie foreslått i å undersøke muligheten for reduksjon i tykkelse av stålet når et rørstykke er pålagt tykk belegg.

Contents

List of Figures

List of Tables

Abbreviations

LPF	**L**oad **P**roportionality **F**actor
FJC	**F**ield **J**oint **C**oating
CFR	**C**oating **F**ield **R**epair
FE	**F**inite **E**lement
AE	**A**sphalt **E**namels
PIP	**P**ipe **I**n **P**ipe
SMYS	**S**pecified **M**inimum **Y**ield **S**trength
BOEPD	**B**arrels **O**f **O**il **E**quivalent **P**er **D**ay
OD	**O**uter **D**iameter
ID	**I**nner **D**iameter
DOF	**D**egree **O**f **F**reedom
PLF	**L**oad **P**roportionality **F**actor
PSI	**P**ound per **S**quare **I**nch
PNM	**P**arallel **N**etwork **M**odel

Symbols

P_e	External Pressure	[Mpa]
P_i	Inner Pressure	[Mpa]
P_{el}	Plastic Collapes Capasity	[MPa]
P_{pl}	Elastic Collapse Capasity	[MPa]
P_c	Collaps Capasity	[Mpa]
σ_u	Ultimate Stress	[MPa]
σ_y	Yield Stress	[MPa]
E	Young's modulus	[MPa]
ν	Poissons ratio	
ϵ_y	Yield Strain	%
ϵ_u	Ultimate Strain	%
F_{ec}	End-Cap Force	[N]
D_{min}	Minimum Diameter	[mm]
D_{max}	Maximum Diameter	[mm]
D_{av}	Average Diameter	[mm]
A_i	Inner Cross-Sectional Area	[mm^2]
A_e	External Cross-Sectional Area	[mm^2]
S	Effective Axial Force	[N]
N	True Axial Force	[N]

Chapter 1

Introduction

1.1   Background

Deepwater oil and natural gas is becoming increasingly important to the global hydrocarbon supply shown by a study done by Douglas Westwood [1], and illustrated in Figure(1.1). This results in the growing need for a better understanding of subsea pipeline collapse capacities.

When a pipe is laid at large depths it is required that the wall thickness is sufficient to withstand the outer pressure. To protect the pipeline from the harsh environment and ensure reliable flow operation, different coating solutions are introduced. Today's design formulas are not accounting for the coating on the pipeline. Such a coating will on one side increase the outer diameter and thereby the loads, but will also to some extent increase the capacity

1.2   Objectives of the study

Existing design formulas for collapse are neglecting the effect of pipeline coating. It is therefore of great interest to the industry to investigate if todays practice of neglecting the coating is acceptable. The objective of this project is to study the effect of coating on the collapse capacity of subsea pipelines. In order to include coating parameter by FE-analysis a suitable material model for the coating has to be developed and
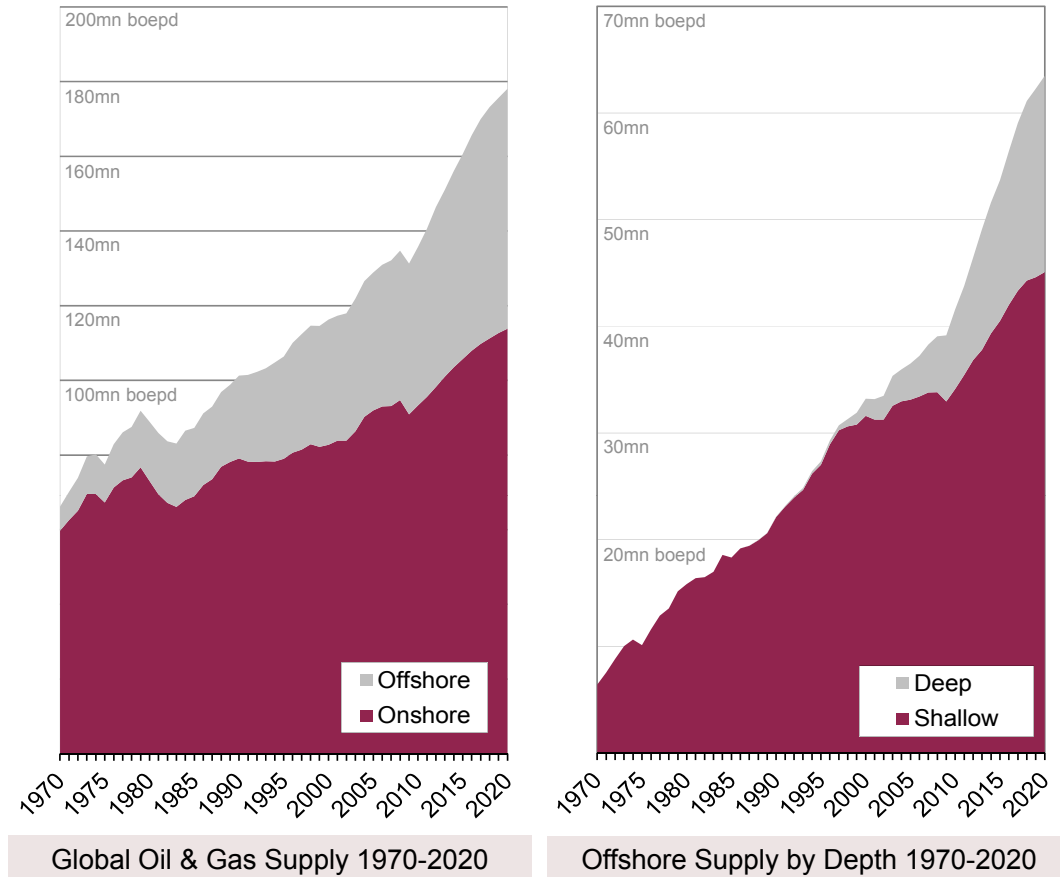
FIGURE 1.1: An outlook for the global deepwater oil and gas supply. Curtesy of Douglas Westwood [1]

included in ABAQUS FE- program. The result must then be compared to both a uncoated pipeline collapse and analytical predictions of pipeline collapse.

1.3 Structure of thesis

In the first part of this thesis (Chapter 2 and 3) some background information is presented regarding the collapse of pipelines with relevant analytical formulations. Followed after *Pipeline Collapse* some information is provided on offshore coating and its applications. Second part of this thesis (Chapter 4) describes the development of the FE-model where coating is left out. This is done so the model can be verified with the analytical formulations and the collapse equation used in DNV-OS-F101 [2]. Following this in the third part (Chapter 5 and 6) the FE- model is developed further including coating where parameter such as thickness, Young's modulus (E), yield

values and ovality are studied. Finally the findings are discussed and the conclusions made, followed by references and appendix.

Chapter 2

Pipeline Collapse

2.1 Introduction

Generally the main design load of pipelines installed on land and shallow waters is internal pressure and the failure mode is burst. By contrast, moving into deeper waters the primary load is external pressure, hence the failure mode is collapse [3] [4]. The collapse of a pipeline will be at the most critical limit when the pipe is empty, evidently as pressure difference between inner and outer pipe wall is at its largest value [3]. This situation is most relevant when the pipeline is installed. All pipelines are installed empty, due to the reduction of weight to the pipeline itself, but also to the equipment [5]. In the recent years a vast amount of research and many papers written on the subject and therefore this chapter will be a brief introduction on the subject of collapse. An extensive coverage of the collapse theory is covered in [6]

2.2 Analytical Formulations

When a pipe is subjected to external pressure, it will cause an compressive hoop stress in the pipe wall. As an consequence the stability of the cross section of the pipe is dependent of the yield strength and hoop stiffness. Thus collapse capacity of a pipeline subjected to external overpressure is assumed to be an combination of the plastic and elastic collapse capacity pressure [5]. The plastic and the elastic equations can be expressed as:

Plastic collapse pressure:

$$P_{pl} = 2 \cdot f_y \frac{t}{D} \tag{2.1}$$

Where f_y is the yield strength, t is the pipe thickness and D is the pipe diameter.

Elastic collapse pressure:

$$P_{el} = \frac{2E}{1 - \nu^2} \left(\frac{t}{D} \right)^3 \tag{2.2}$$

Where E is the *Modulus of elasticity* or *Young's modulus*, ν is the *Poissons ratio*, t is the pipe thickness and D is the pipe diameter.

Collapse is an highly complicated matter as it is an instability issue [5]. The collapse prediction formulas are not only functions of Equation(2.1) and (2.2), but also the ovality of the pipeline, witch is expressed as:

Ovality:

$$f_0 = \frac{D_{max} - D_{min}}{D_{avg}} \tag{2.3}$$

Where D_{max}, D_{min} and D_{avg} is the maximum, minimum and average diameter respectively. A sketch of an ovalised pipe is shown in Figure(2.3).There exists however a second definition of *Ovality* found in literatures:

$$f_0 = \frac{D_{max} - D_{min}}{D_{max} + D_{min}} \tag{2.4}$$

The equation used in DNV-OS-F101 [2] and the one considered during this text is Equation(2.3).

There tree equations that describes the collapse capacity of a pipeline and that are widely in use today are *Timoshenko*, *Shell* and *Haagsma* equation. [6].

Timoshenko equation:

$$(P_c - P_{el}) \cdot (P_c - P_{pl}) = 1.5 \cdot P_c P_{el} f_0 \frac{D}{t} \tag{2.5}$$

P_{el} is the elastic collapse pressure, P_{pl} is the plastic collapse pressure and the f_0 is the ovality.

Shell equation:

$$P_c = \frac{P_{pl} P_{el} g}{\sqrt{P_{el}^2 + P_{pl}^2}} \tag{2.6}$$

Where P_{el} is the elastic collapse pressure, P_{pl} is the plastic collapse pressure and g is given as:

$$g = \sqrt{\frac{1 + \left(\frac{P_{pl}}{P_{el}}\right)^2}{\left(\frac{P_{pl}}{P_{el}}\right)^2 + f^{-2}}} \tag{2.7}$$

where f is given as:

$$f = \frac{1}{\sqrt{1 + \left(0.5 \cdot f_0 \frac{D}{t}\right)^2}} - 0.5 \cdot f_0 \frac{D}{t} \tag{2.8}$$

The third equation and the one that is used in DNV-OS-F101 [2] and that will be considered during this text is given as:

Haugsma equation:

$$(P_c - P_{el}) \cdot (P_c{}^2 - P_{pl}{}^2) = P_c P_{el} P_{pl} f_0 \frac{D}{t} \tag{2.9}$$

P_{el} is the elastic collapse pressure, P_{pl} is the plastic collapse pressure and the ovality f_0 as defined in equation (2.3).

Figure(2.1) is a plot of the plastic, elastic together with the *Haagsma*, *Shell* and *Timoshenko* equations.
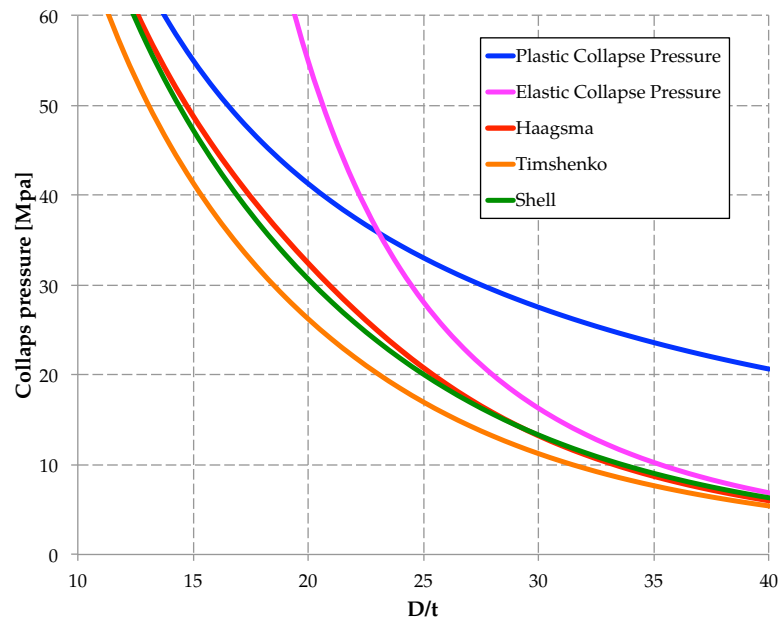
FIGURE 2.1: Collapse resistance as a function of diameter to thicknes for plastic, elastic, *Haagsma*, *Shell* and *Timoshenko* equations. Yield strenght is set to 450 MPa and an ovality of 0.005 (0.5%).

2.2.1 Critical Diameter to Thickness Ratio

The plot of *Haagsma* equation in Figure(2.1) is actually a "best fit" of the elastic and plastic curves if the pipe is perfectly round i.e. ovality = 0 as shown in Figure(2.2). It is assumed that for pipes with any given ovality and diameter over thickness ratio ($\frac{D}{t}$) around 20-25, there exist an critical point where the collapse capacity will deviate at its highest value from the best fit curve. From Figure(2.1) the pressure difference for *Haagsma* and the point where the elastic and plastic curves meet one can measure approximately 10 MPa, however it is noted that the exact point does not necessarily represent the critical $\frac{D}{t}$.
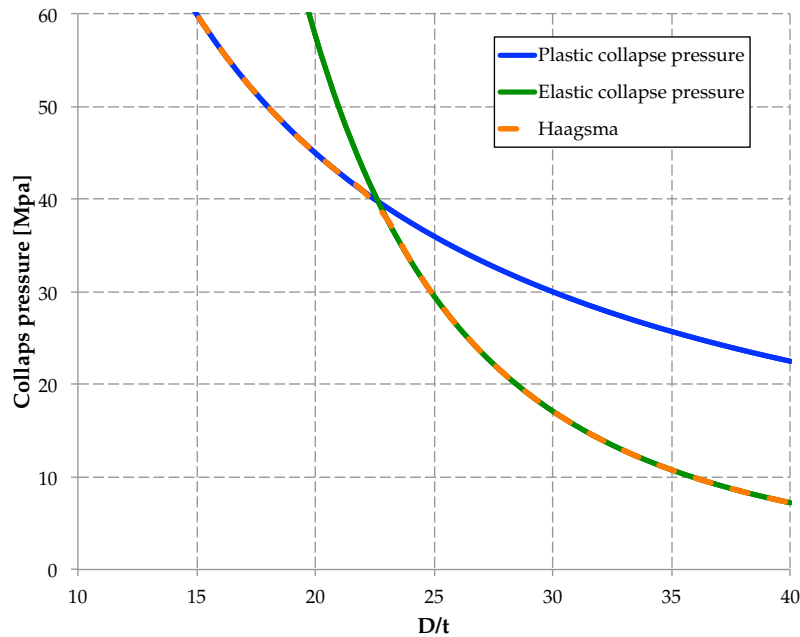
FIGURE 2.2: Collapse equations with zero ovality.

In order to clearly visualise the critical area Equation(2.9) has been evaluated with ovality of 0%, 0.5 % 1% and 2% for $\frac{D}{t}$ of 10, 15, 20, 25 and 45. The result are plotted in Figure(2.4) following Equation(2.10).

$$\frac{P_c(\frac{D}{t}, f)}{P_c(\frac{D}{t}, f_0)} = C \qquad , \tag{2.10}$$

$$C = \begin{cases} < 1 & : f_0 < f \\ > 1 & : f_0 > f \end{cases}$$

Figure(2.4) illustrates that $\frac{D}{t}$ of 25 has the highest value. I.e. for any ovality, $\frac{D}{t}$ of 25 will deviate most from its zero ovality path. The theory of critical $\frac{D}{t}$ will be discussed further in Chapter(4).
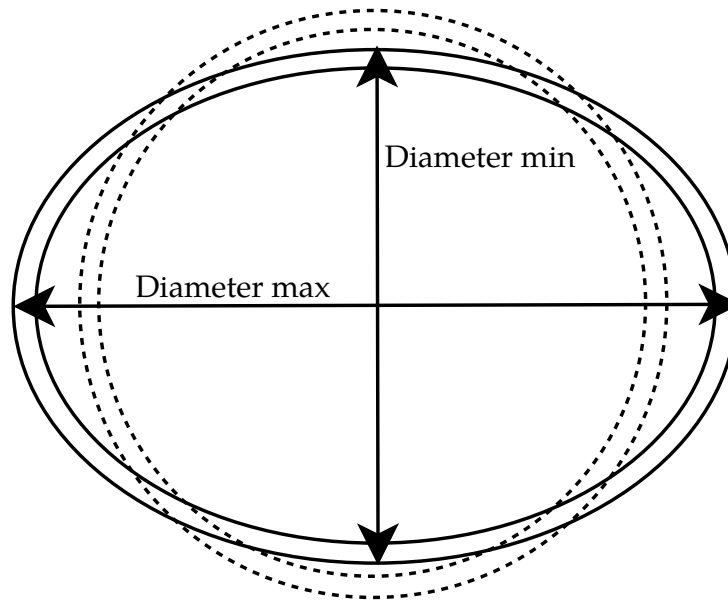
FIGURE 2.3: Pipeline ovality.
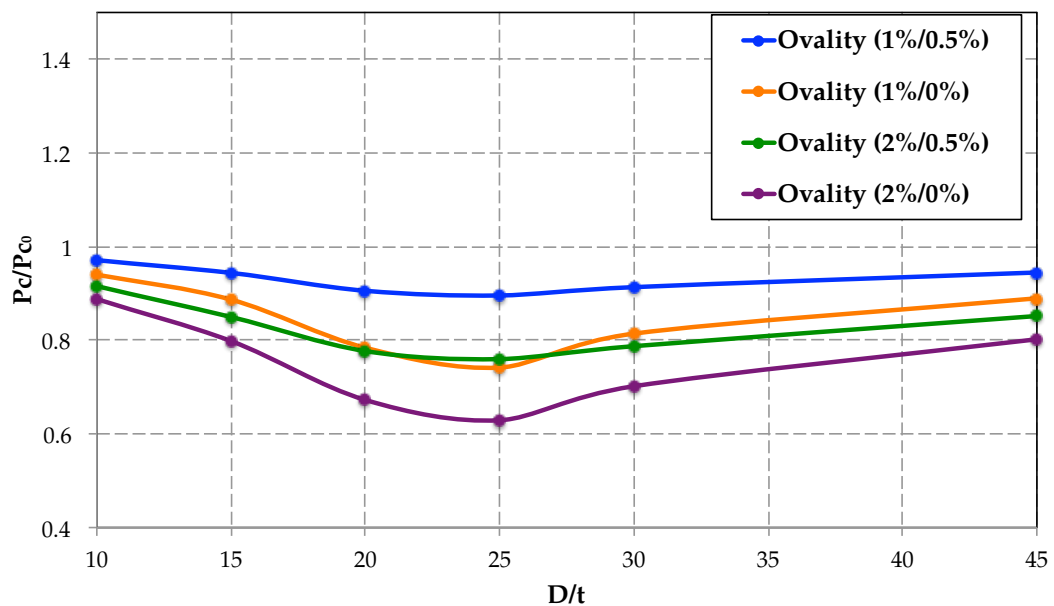
FIGURE 2.4: Plot of collapse values from Equation(2.10), showing pipe with $\frac{D}{t}$ of 25 with peak value for all ovality comparison.

Chapter 3

Offshore Coating

3.1 Introduction

A primary objective and the most important factor for applying external coating on a pipeline is to prevent it from corrosion. In addition to corrosion prevention, anti corrosion coating can be designed to give mechanical protection for the pipeline during installation and operation. Such a coating can also be combined with concrete weight coating for negative buoyancy and mechanical protection . In addition to protecting the pipeline material, thermal insulation may be used for flow assurance purposes [7]. Over the past 50 years the coating industry has coated the oil and gas pipelines with a variety of coatings. Such coatings are coal tar or asphalt enamels (AE), tapes of polyolefin material, double layer extruded polyethylene coatings, single or dual layer fusion bonded epoxy (FBE) coatings, three or multi-layer polyolefin coatings, etc [8]. In this chapter the above coating applications will be discussed followed by mechanical formulations.

3.2 Coating Application

Pipeline coating can be divided into five main type of applications with each its intended purpose described in the following sub chapters.

3.2.1 Anti-Corrosion

External coating for prevention of corrosion of pipelines are applied to pipe lengths individually at a dedicated coating mil/plant. The types of coating and wrapping that are used are mainly plastic based materials due to their superior corrosion resistance [9], but as mentioned earlier tar or AE are also used. The three main types of coating applications are extrusion, spraying and spiral wrapping method.

Firstly before adding the coating a primer needs to be laid in order for the coating to stick. Normally the primer is fusion bonded epoxy (FBE) or butyl that is applied under a topcoat containing one or several layers coating material designed for the specific pipeline project. Type of the material and the numbers of layers is dependent of the cost and the amount of protection the pipeline needs [8].

1. Fusion Bonded Epoxy
2. Copolymer Adhesive
3. Polypropylene
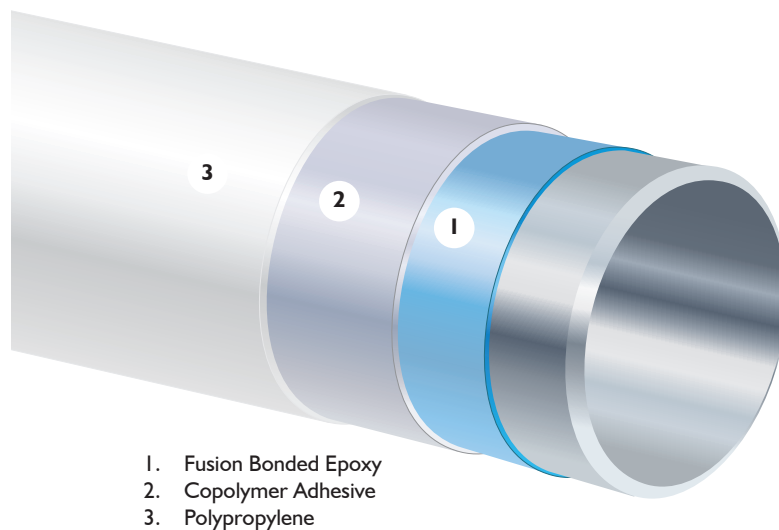
FIGURE 3.1: Three Layer Polypropylene Coating (3LPP). Curtesy of BrederoShaw

3.2.2 Flow assurance

Thermal Insulation is a key to ensure reliable operation of subsea flowlines [10]. There are two main approaches to insulate pipelines for subsea structures, Pipe-in-Pipe (PIP) insulation and wet insulated pipe[11].

Pipe-in-Pipe

This application consist of an inner and outer steel pipe with insulation material filled
in the annular space between them. PIP insulation is often called 'dry' insulation as
the foam is protected from the water by the outer pipe, and as a consequence can
be constructed with a low mechanical strength and high insulating values. The most
common used material is polyurethane foam. PIP insulated flowlines is heavier and
have a more expensive construction than of wet pipe insulation but can on the other
hand achieve low U-values and high insulation performance [11].

Wet insulated pipe

Wet insulated pipe is the most commonly used thermal insulation for deepwater flow-
lines. In this application, steel pipes are directly insulated with a syntactic foam
material, normally polypropylenes. The insulation generally do not have any protec-
tive cover. The low-density hollow microspheres in the composite reduce both the
weight and thermal conductance of the coating [11].

1. Fusion Bonded Epoxy
2. Adhesive
3. Solid PP
4. PP Insulation
5. Outer Shield
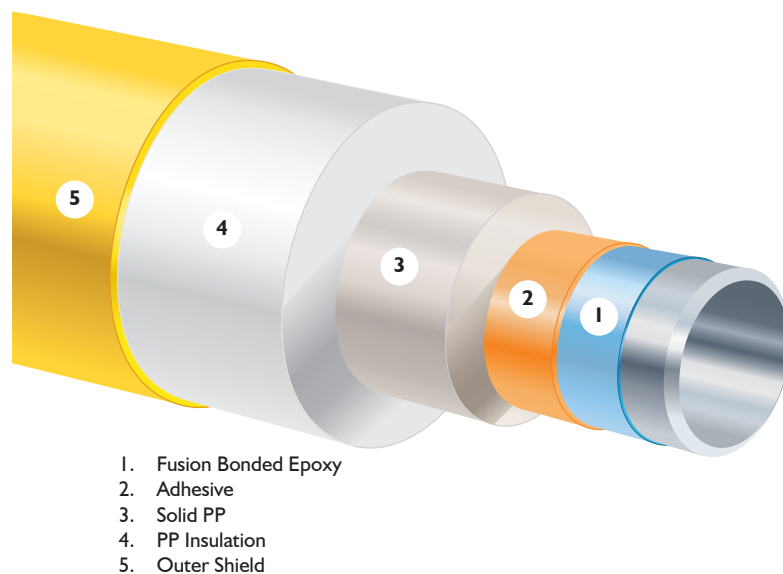
FIGURE 3.2: Wet insulated pipe (Thermotite ®). Curtesy of BrederoShaw

3.2.3 Protective and Weight

Many submarine pipelines are coated with concrete weighted coating to ensure seabed stability. A typical concrete density is 2400 kg/m^3, but can be increased by adding a heavier aggregate such as iron ore, barytes etc. It is important for the aggregate to withstand the sulphate in the seawater [12]. The thickness of the concrete is also varied and can be seen in the region of 25-230 mm [13].

1. Anti-Corrosion Coating
2. Reinforced Concrete
3. Outer Wrap
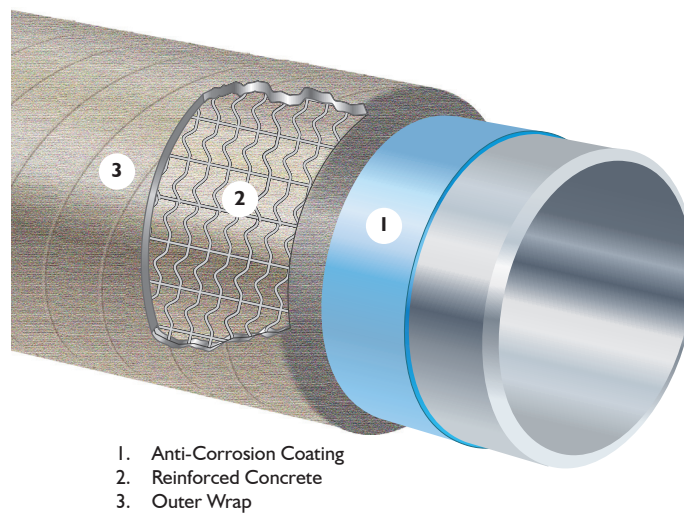
FIGURE 3.3: Concrete weight coating. Curtesy of BrederoShaw

3.2.4 Internal coating

There are three main purposes for a pipeline to be coated internally; Improve flow by reducing friction induced drag by the pipe wall, anticorrosion provided before construction and helping to detect faults to the inner wall of the pipe. The coating thickness is in the range of 30-150 μm [9], hence it is too small to make any impact on the collapse capacity and will not be considered in this text.

3.2.5 Field joint coating

Subsea pipeline installation is performed by specialised lay-vessels, with several possible methods. The most common methods being S-lay, J-lay and reeling. For the latter method the pipe sections are connected and reeled to drums onshore and hence not relevant to field joint coating. During installation of a pipeline by S-lay and J-lay

method, each pipe section are welded and sealed with coating at the lay vessel, hence the name Field Joint Coating [12]. At the construction and coating of the pipe, section ends are left uncoated at the standard length of 150 mm [9] The ends are however painted with anticorrosion paint for the steel not to be left totally unprotected. An illustration of the coating layers included in field joint coating is shown in Figure(3.4).
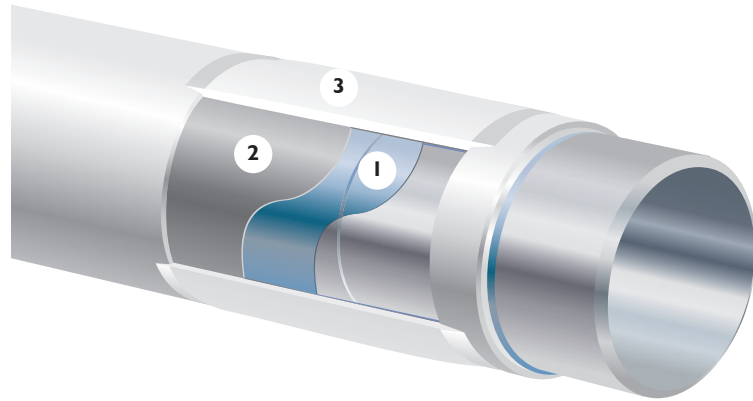
1. Fusion Bonded Epoxy
2. Copolymer Adhesive
3. Solid Injection-Moulded Polypropylene

FIGURE 3.4: Field joint coating (FJC). Curtesy of BrederoShaw

BREDERO SHAW

3.3 Mechanics of Coating

As a coated pipeline consist of a minimum of two materials it would be appropriate to obtain that material quality and hence the behaviour (stress-strain curve) of the materials used. In contrast to steel, modelling coating materials can be a complicated matter let alone obtaining the true values from manufacturers. Stress-strain theory of Polypropylene solid and foam are presented in Chapter(5.2.2)

When considering the failure mode collapse, study and tests has shown that the initiation of collapse in pipelines starts at a *compressive* strain level in the range of 0.2-0.3 % [4]. In some analysis the assumption of coating material model above would be wrong. However in collapse analysis a strain level of 0.2-0.3 % in the steel would be in the elastic area of the coating as shown in Figure(3.5) and (3.6) if Polypropylene is used. Hence the elastic modulus (E) and yield stress (σ_y) would be more important than obtaining the true plastic behaviour of the coating. Stating this, a simple theory is formulated to look at the *compressive* stress intensity in a coated steel section when subjected to outer pressure. Also a theory of serial resistance is presented looking at the collapse prediction like a electrical circuit.
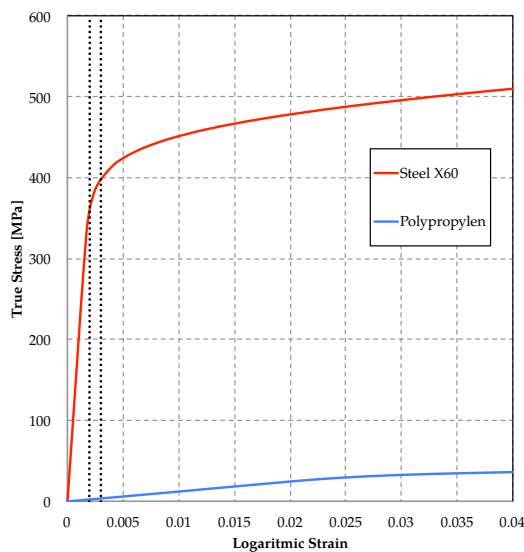
FIGURE 3.5: True stress and loaritmic strain curve for steel and Polypropylen, where the indicated area between 0.2-0.3 % is the likely collapse strain
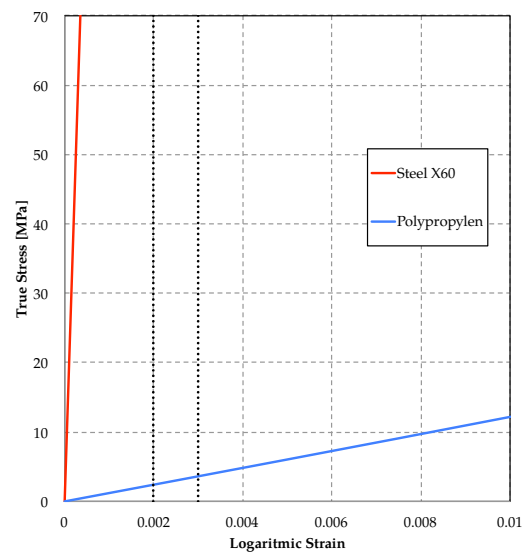
FIGURE 3.6: Enlarged area off collaspe in the stress and strain curve for steel and polypropylen showing the affected elastic area of the curve.

3.3.1 The Theory of Hoop Stress
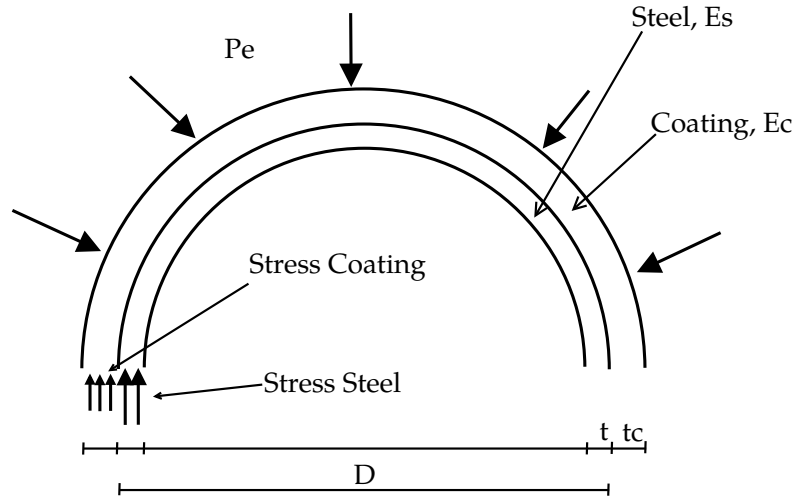
FIGURE 3.7: Stress distribution on half section of a pipe with coating, where the subscript c and s are coating and steel respectively. E is Elastic modulus, t is the tickness and D is the steel pipe diameter.

By considering static equilibrium for the half pipe in Figure(3.7) we can express the forces in y- direction from *Newton's second law*:

$$\sum F = 0 \tag{3.1}$$

$$F_c + F_s = F_e \tag{3.2}$$

$$\sigma_c A_c + \sigma_s A_s = P_e A_e \tag{3.3}$$

$$\tag{3.4}$$

Where F_c and F_s is the force on the coating and steel respectively. Since we are working in 2-D the areas (L^2) is transformed to lengths (L).

$$\sigma_c(2t_c) + \sigma_s(2t) = P_e(D + 2t_c) \tag{3.5}$$

By considering the coating and the steel to have an equal displacement we get:

$$\epsilon_c = \epsilon_s \tag{3.6}$$

$$\sigma_c = \frac{E_c}{E_s}\sigma_s \tag{3.7}$$

Inserting Equation(3.7) to (3.5) we can express the non dimensional steel hoop stress in Equation(3.10):

$$\frac{E_c}{E_s}\sigma_s(2t_c) + \sigma_s(2t) = P_e(D + 2t_c) \tag{3.8}$$

$$\sigma_s 2t\left(\frac{E_c}{E} \cdot \frac{t_c}{t} + 1\right) = P_e(D + 2t_c) \tag{3.9}$$

$$\frac{\sigma_s 2t}{P_e D} = \frac{1 + \frac{2t_c}{D}}{\left(\frac{E_c}{E} \cdot \frac{t_c}{t} + 1\right)} \quad \text{or} \quad \frac{1 + 2\frac{t_c/t}{D/t}}{\left(\frac{E_c}{E} \cdot \frac{t_c}{t} + 1\right)} \tag{3.10}$$

Unarguably steel elasticity is much higher than coating elasticity and hence when $\frac{E_c}{E} \Rightarrow 0$, Equation(3.10) $\Rightarrow 1 + \frac{2t_c}{D}$. This is not surprising as adding $\frac{2t_c}{D}$ to the hoop stress is intuitive when pipe hoop stress (without coating) found in many literatures is given as:

$$\sigma_s = \frac{P_e D}{2t} \tag{3.11}$$

However Equation(3.10) does surprise when $\frac{E_c}{E} = \frac{t}{2D}$ as seen with the green line in Figure(3.8), also yields the constant value of 1 for any coating thickness.
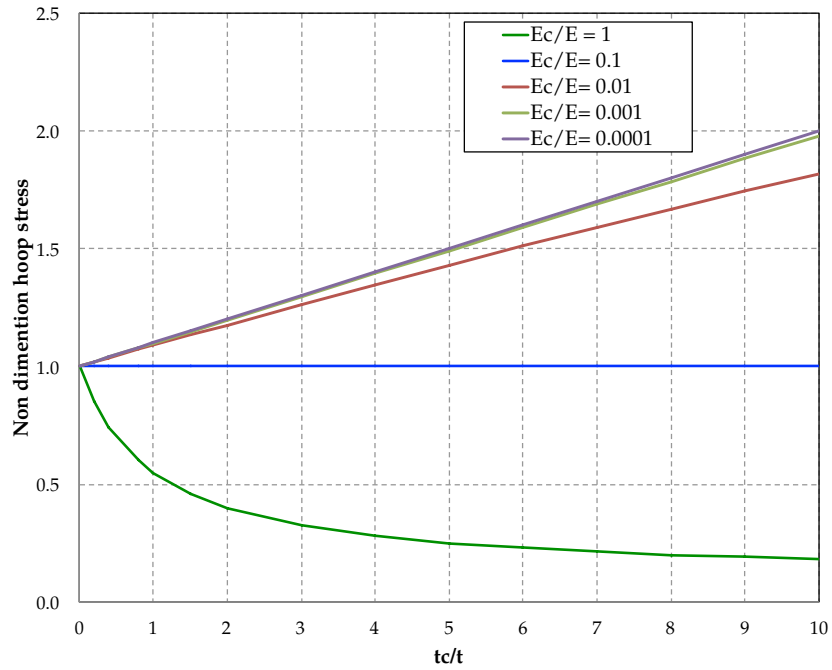
FIGURE 3.8: Shows the non dimentional hoop stress (Eq.3.10) induced in the steel pipe ($\frac{D}{t} = 20$) by the effect of outer pressure with different t_c/t, plotted for several E_c/E

Considering Polypropylene as the coated material with a elasticity of 1140-1550 MPa and steel elasticity of $2.0 \cdot 10^5$ MPa [14], we get $\frac{E_c}{E}$ of 0.0057-0.0077. This results in 25% increase in steel hoop stress when the coating thickness is the double size of the steel thickness as seen in Figure(3.8). This statement is however not directly related to the collapse capacity of the pipeline as the coating strength is neglected.

3.3.2   The Theory of Serial Resistance

Looking at the collapse prediction of a coated pipeline like a electrical circuit with two resistors connected in series the equivalent resistance is as simple as:

$$R_{eq} = R_1 + R_2 \tag{3.12}$$

Now inserting the collapse resistance for the electrical resistance we get:

$$P_{tot} = P_{ct} + P_{st} \tag{3.13}$$

Where the P_{ct} and P_{st} is the coating and steel collapse resistance respectively evaluated with Equation(2.9). Hence the coating layer and the steel pipe is considered as two separate pipes as shown in Figure(5.12)
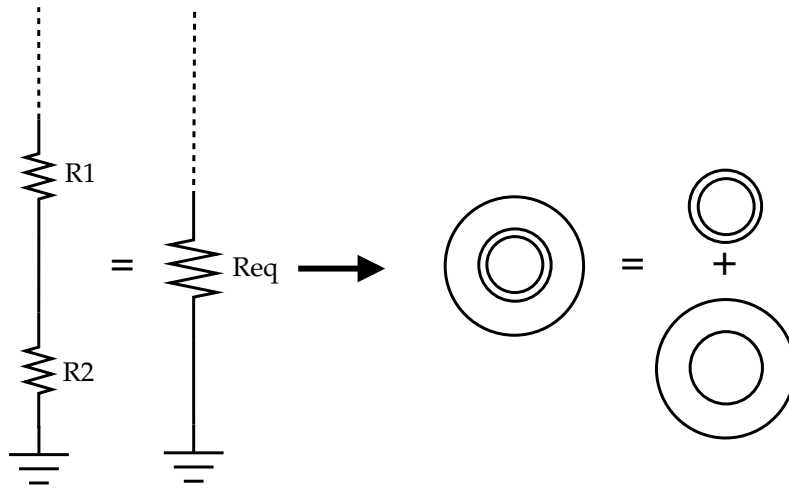
FIGURE 3.9: Equivalent physical systems for the theory of serial resistance.

Chapter 4

Uncoated FE-model

4.1   Introduction

The FE-model was built in the ABAQUS CAE 6.13 Finite Element software by the use of C3D8R (**c**ontinuum, **3D**, **8**-node elements with **r**educed integration). This model was made as a small section of a long pipe. The objective of the making and analysis of the pipe section without coating has been to verify its behaviour when subjected to external pressure, by comparing the data to analytical formulations. In order to compare the collapse capacity of the model to analytical prediction a number of 18 different cases has been investigated with different yield strength, diameter to thickness ratio and ovality. In the next chapter the effect of coating has been included.

4.2   3D-Model

The 3D model for this analysis was built using the modules in ABAQUS CAE as shown in Figure(4.1). Certain aspects of the input data has been explained in the following subchapters.
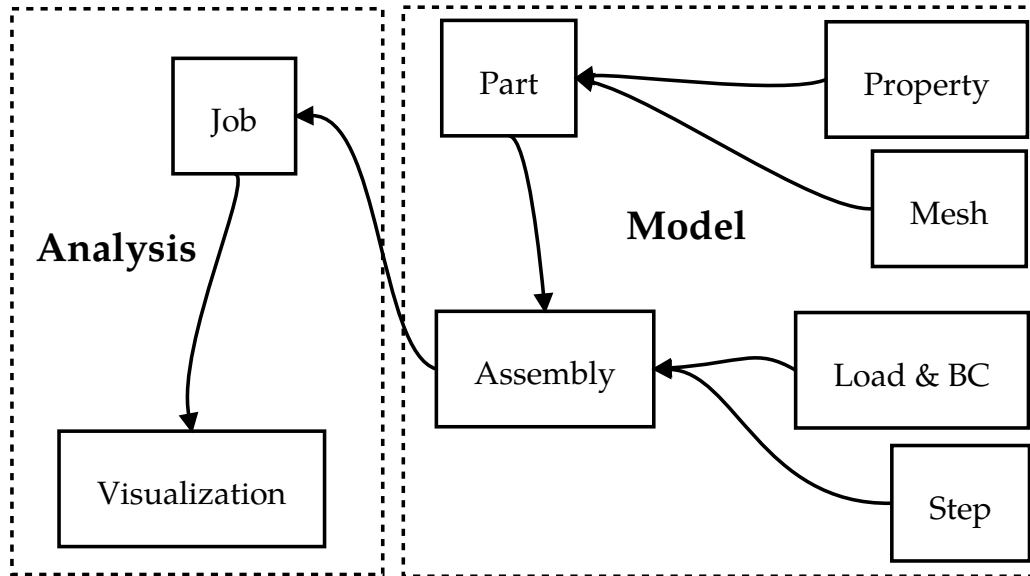
FIGURE 4.1: This FE-model was build using the modules in ABAQUS CAE shown in this figure.

4.2.1 Ovality

The pipe was drawn by a three point ellipse (center, D_{max} and D_{min}) where the D_{max} and D_{min} was inserted by coordinates and then extruded axially. Normally the D_{av} is an average of eight measurements of the pipe diameter [2], however for simplification in drawing the model it was defined as:

$$D_{av} = \frac{D_{max} + D_{min}}{2} \tag{4.1}$$

Hence the Equation(2.3) for this model is transformed to:

$$f_0 = \frac{2 \cdot (D_{max} - D_{min})}{D_{max} + D_{min}} \tag{4.2}$$

By assuming two variables in Equation(4.2), the ellipse can be drawn.

4.2.2 Steel Material Model

The material behaviour data for the pipe subjected to high pressure thus undergoes large plastic deformations was required in this analysis. In order to insert the true

stress and plastic logarithmic strain values in ABAQUS the following approach has been applied.

$$\epsilon_{eng} = \frac{\Delta l}{l_0} \quad , \quad \sigma_{eng} = \frac{F}{A_0} \tag{4.3}$$

The above equations are both *engineering* values, and it is assumed:

$$\epsilon_y = 0.5\% \quad \text{and} \quad \epsilon_u = 10\% \tag{4.4}$$

Transforming to *logarithmic* strain and *true* stress yields:

$$\epsilon_{ln} = \ln(1 + \epsilon_{eng}) \quad , \quad \sigma_{tr} = \sigma_{eng} \cdot (1 + \epsilon_{eng}) \tag{4.5}$$

$$\epsilon_{ln,u} = \ln(1 + \epsilon_u) \quad , \quad \sigma_{tr} = \sigma_{eng} \cdot (1 + \epsilon_u) \tag{4.6}$$

The definition states two points on the true stress and logarithmic strain curve, true yield and true ultimate values. One way of formulating the Ramberg-Osgood stress-strain curve is by the two parameters α and n:

$$\epsilon_{ln} = \frac{\sigma_{tr}}{E} \left(1 + \alpha \cdot \left(\frac{\sigma_{tr}}{\sigma_y \cdot 1.005} \right)^{n-1} \right) \tag{4.7}$$

Where α and n are defined as:

$$\alpha = E \cdot \frac{\ln(1.005)}{\sigma_y \cdot 1.005} - 1 \tag{4.8}$$

$$n = \frac{\ln \left(\ln(1.1) - \frac{\sigma_u \cdot 1.1}{E} \right) - \ln \left(\ln(1.005) - \frac{\sigma_y \cdot 1.005}{E} \right)}{\ln \left(\frac{\sigma_u \cdot 1.1}{\sigma_y \cdot 1.005} \right)} \tag{4.9}$$

The logarithmic strain as a function of true stress is then:

$$\epsilon(\sigma) = \alpha \cdot \frac{\sigma}{E} \cdot \left(\frac{\sigma}{\sigma_y \cdot 1.005} \right)^{n-1} \tag{4.10}$$

The values for Equation(4.10) was calculated with values of three relevant steel quality listed in Table(4.1) with a spread sheet and inserted in ABAQUS.

4.2.3 Boundary Conditions

The initial condition used for this model are both directional displacement restriction and kinematic coupling. Kinematic coupling in this case eliminates all degrees of freedom of a group of nodes and couple their motion to the motion of a reference node. The reference node is normally referred to as *master* node, and the coupled nodes are called *slave* nodes . The elements used for this model (C3D8R) had only three DOF and in order to constraint the model in all six DOF the following actions was taken:

1. Reference node restrained in x, y and all rotational DOF.

2. Two nodes are restrained in x and z direction with a kinematic coupling to the reference node as illustrated in Figure(4.2).

3. Two nodes are restrained in y and z direction with a kinematic coupling to the reference node Figure(4.2).

4. In the same transverse plane as nodes above, all nodes _except_ the nodes above restrained in in z-direction with kinematic coupling to the reference node as illustrated in Figure(4.3).

5. In the other transverse plane, all nodes was constrained in z-direction

By choosing the following nodes as stated above and illustrated in Figure(4.2) and (4.3) the model is then restraints in all six DOF, but free to collapse.

4.2.4 Axial Force Consept

The concept of effective axial force is a simplification of how both internal and external pressure impact the pipeline behaviour hence it is very important consideration for pipeline design [15]. The topic is extensively covered in [16]. However a short description is included herein. By considering a section of a pipeline submerged in water. The forces acting on the surface of the pipe is illustrated in Figure(4.4). When applying statical equilibrium for the section we get:

$$\sum F = S - N - F_{ec} = 0 \tag{4.11}$$
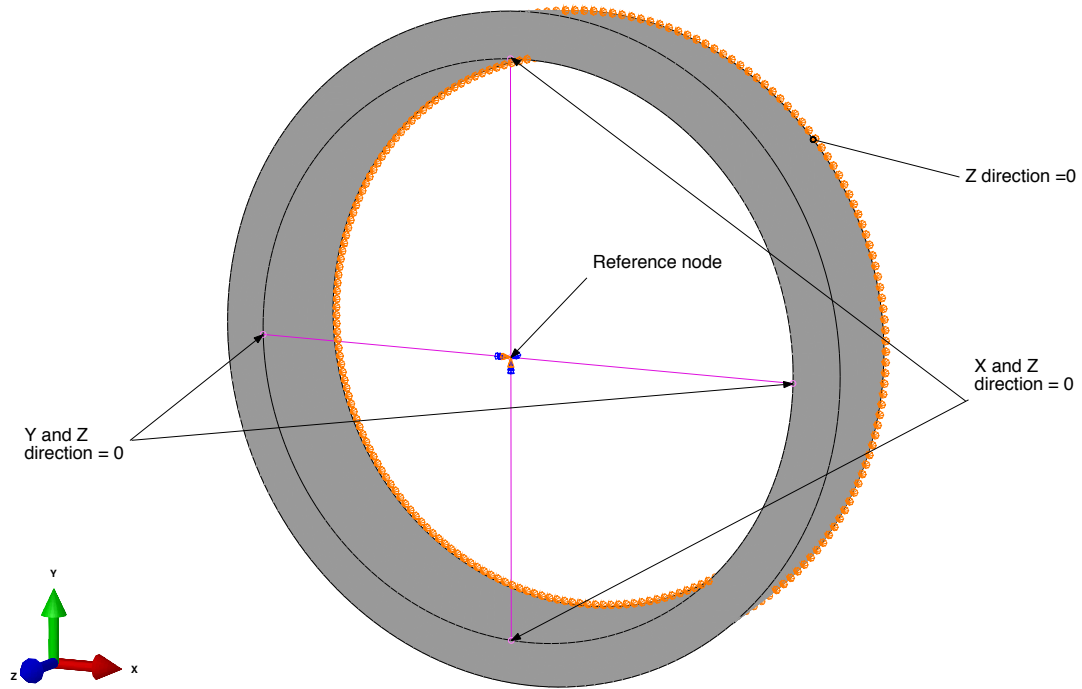
FIGURE 4.2: Boundary conditions for the model, where two dobbel nodes are connected with kinematic coupling to the reference node. The reference node is restrained in x, y and all rotational DOF. The orange marks are directional boundary conditions with restrictions in z- direction

N is the true axial force found by integrating the axial stresses over the pipe cross section. S is the effective axial force or the resultant force acting on the system. F_{ec} is the end-cap force defined as:

$$F_{ec} = P_i A_i - P_e A_e \tag{4.12}$$

The subscript i and e are *inner* and *outer (external)* respectively. P is pressure an A is the area. By inserting Equation(4.12) into (4.11) we get:

$$S = N - P_i A_i + P_e A_e \tag{4.13}$$
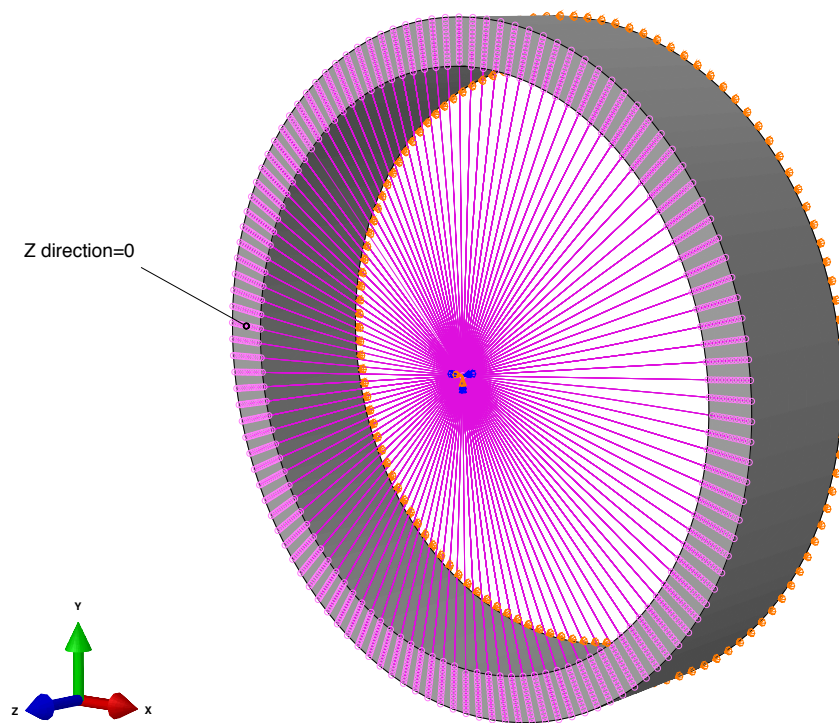
FIGURE 4.3: All nodes except the nodes used in Figure(4.2) are restrained in in z-direction with kinematic coupling to the reference node
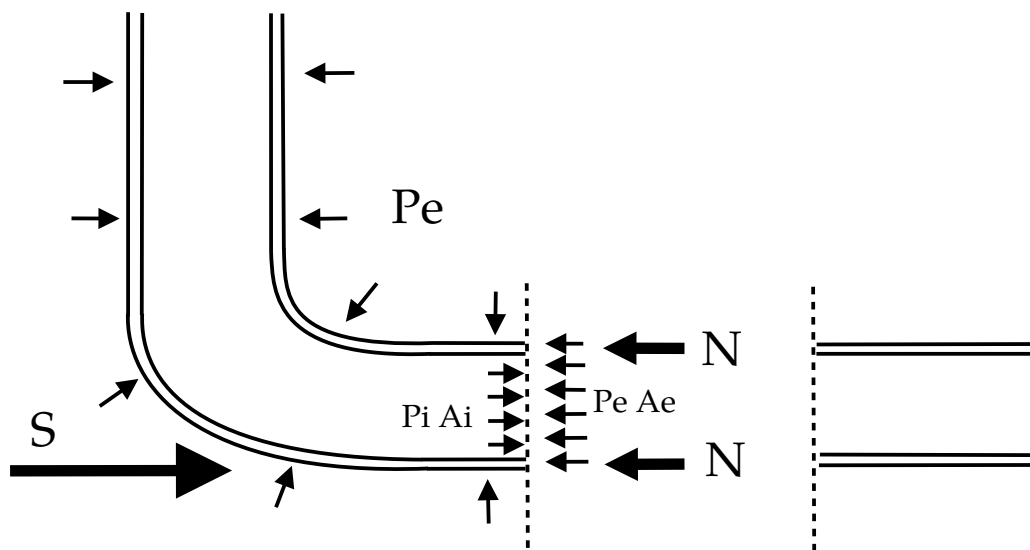
FIGURE 4.4: An illustration of the forces that acts on the section (left section) of a pipe submerged in water. The pipe section is visulalised in 2-D with force simplifications.

In this thesis the pipe section is empty, hence $P_i=0$. If the pipeline is free to expand in one side, the Equation(4.13) results in:

$$N = -P_e A_e \tag{4.14}$$

$$\sigma_{steel} A_{steel} = -P_e A_e \tag{4.15}$$

$$\sigma_{steel} = -\frac{P_e A_e}{(A_e - A_i)} \tag{4.16}$$

The stress σ_{steel} was calculated and inserted as a load on the kinematic coupled area of the cross section.

4.2.5 Arc.-Length Method

Analysis of this geometrically nonlinear static model involves plastic behaviour and large deformation as known for collapse and buckling problems. The load-displacement response yield a negative stiffness as illustrated in Figure(4.5) hence the section release strain energy to remain in equilibrium [17]. The method of **Arc.-Length** or **Modified Riks** is one good approach for solving this type of problems and has been preformed in this thesis. The method involves a load magnitude, in ABAQUS Load Proportionality Factor (LPF) as an additional unknown that solves simultaneously for load and displacement:

$$r(U, \lambda) = \mathbf{K}(U)U - \lambda \mathbf{F} \tag{4.17}$$

Where r is the solution path of the continuous set of equilibrium points, K is the stiffness matrix, λ is the LPF and F is the load, in this case pressure. The load increment is computed using:

$$\lambda = \pm\sqrt{\Delta s^2 - \Delta U_n{}^2} \tag{4.18}$$

Where the arc length is:

$$\Delta s^2 = \frac{\mathbf{F}}{n_{loadsteps}} \tag{4.19}$$

As seen in Figure(4.5) this approach yield a solution regardless of whether the response is stable or unstable.
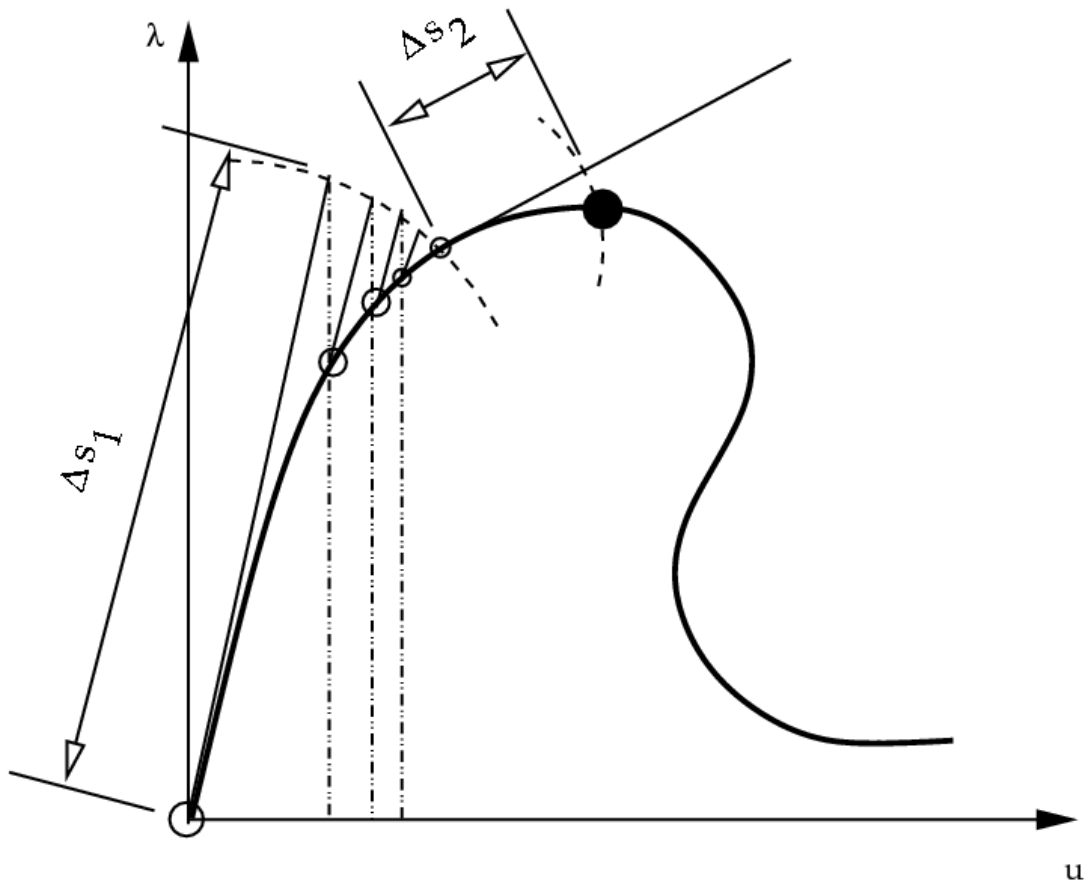
FIGURE 4.5: Load-displacement curve for riks analysis. Δs_1 is the initial step and Δs_2 is the increment

4.3 Results

This model was modified to simulate 18 different specimens, with three steel types, two ovality measures and three diameter to thickness ratio. All specimen has been subjected to external pressure of 60 MPa. The collapse pressure is then as simple as multiplying LPF calculated by ABAQUS at the maximum point of the riks curve shown in Figure(4.6) by the pressure (60 MPa). The result of the FE- analysis is listed in Table(B.1).
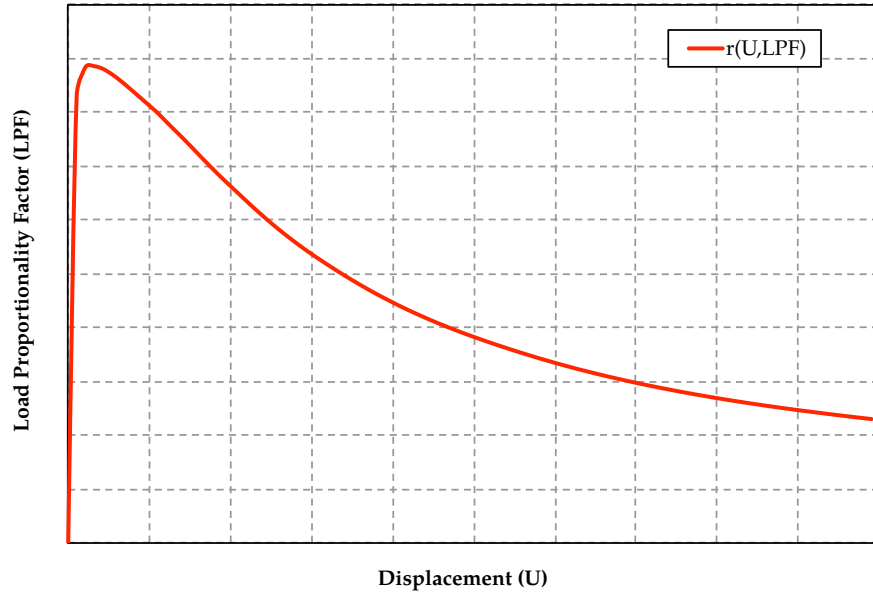
FIGURE 4.6: Load-displacement curve for the FE-model where the maximum value of the LPF is the point of collaspe.

TABLE 4.1: Steel quality used in simulations.

Steel quality.	σ_y [MPa]	σ_u [MPa]	E [MPa]
X60	413.7	517.1	199000
X65	448.2	530.9	199000
X70	482.7	565.4	199000

4.4 Verification

4.4.1 Mesh Convergence

In this model the number of nodes and thereby elements created in the pipe thickness and circumferentially where investigated in order to choose the best configuration with respect to computational time and results. The number of elements created lengthwise was not considered nor investigated due to the constant stress gradient. This is expected as there shouldn't be stress variation in the pipe length as seen in Figure(4.9).

Firstly the circumferential number of elements was determined and with that configuration the number of elements in thickness was determined. The circumferential number of elements are referred to the number of elements per quarter pipe i.e. multiplying by four to get the number for the whole section.

Circumferential number of elements range from 10 to 50 and there was tested with 2, 4 and 6 elements in thickness. It can be seen in Figure(4.10) that the result converge rapidly after 30 elements for all three configurations. Thus the number of 30 elements was chosen. Next the 30 elements circumferentially was used to analyse a range of 3 to 20 elements in thickness seen in Figure(4.11). Again the number of 12 elements was chosen with the same argument as above. The final mesh configuration is illustrated in Figure(4.7) and (4.8)
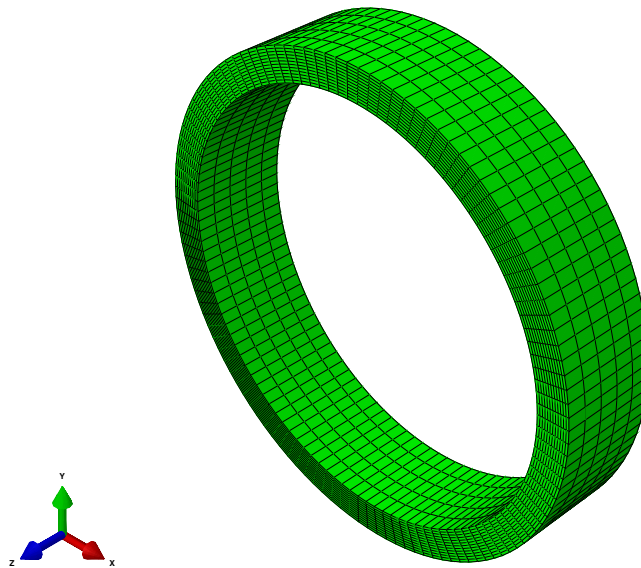
FIGURE 4.7: Mesh of the model in Iso view with the choosen mesh configuration.
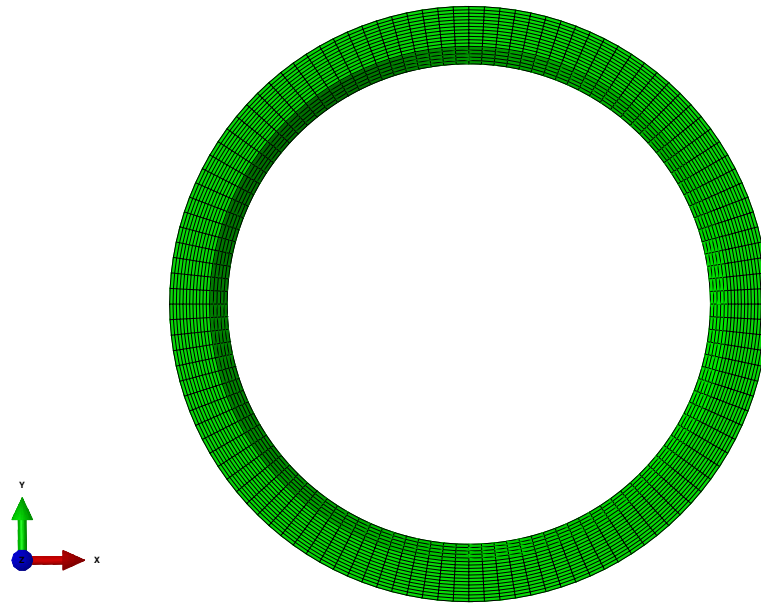
FIGURE 4.8: Mesh of the model in front view.
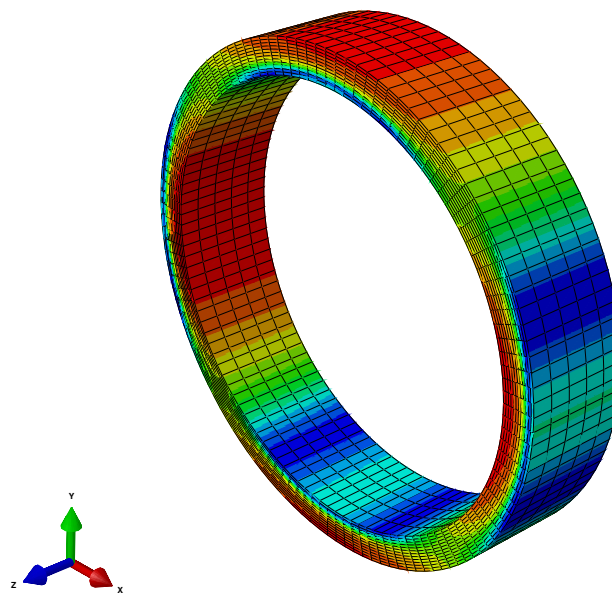
FIGURE 4.9: Stress distribution of the FE- model showing the constant stress gradient in z direction when it is subjected to outer pressure of 60 MPa.
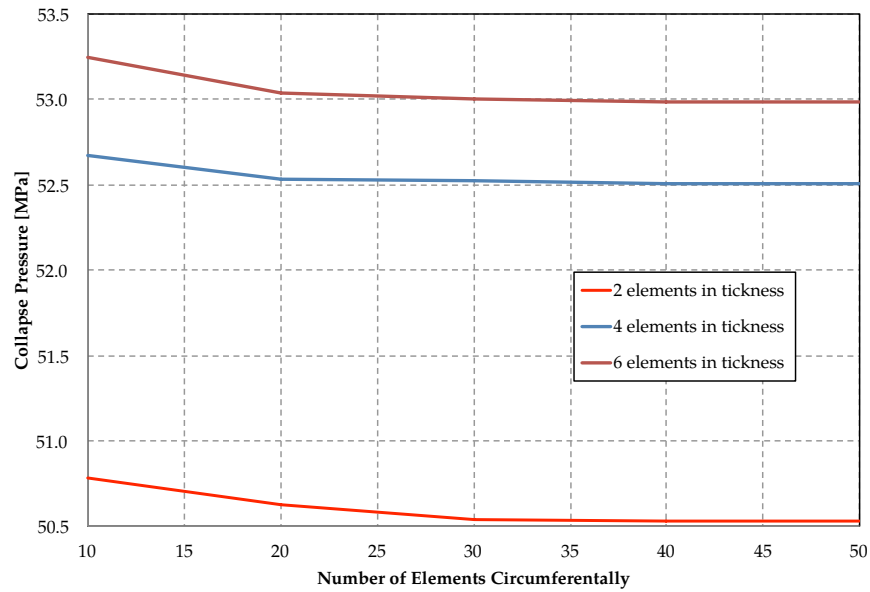
FIGURE 4.10: Mesh convergence circumferentally where three element configuration with respect to thickness was tested.
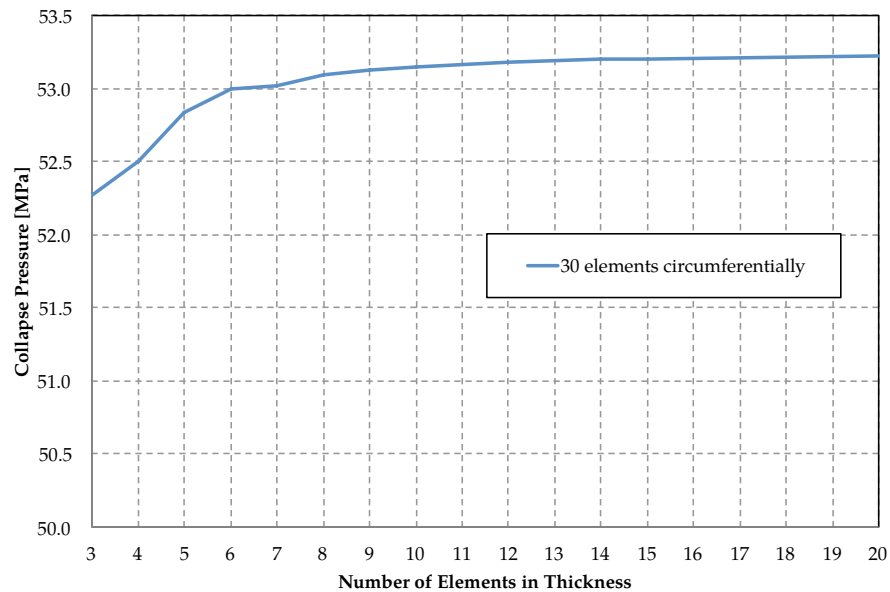
FIGURE 4.11: Mesh convergence in thickness.

4.4.2 Collapse Pressure Comparison

The verification of this model was highly dependant to the collapse prediction that is formulated by the *Haagsma* equation and used in DNV-OS-F101 [2].

The results presented in Table(B.1) and (B.2) and that has been compared to Equation(2.9) has shown a high accuracy where the deviation ranges from 0 to less that 5% of the collapse capacity shown in Figure(4.12), (4.13), (4.14), (4.15) and (4.16)
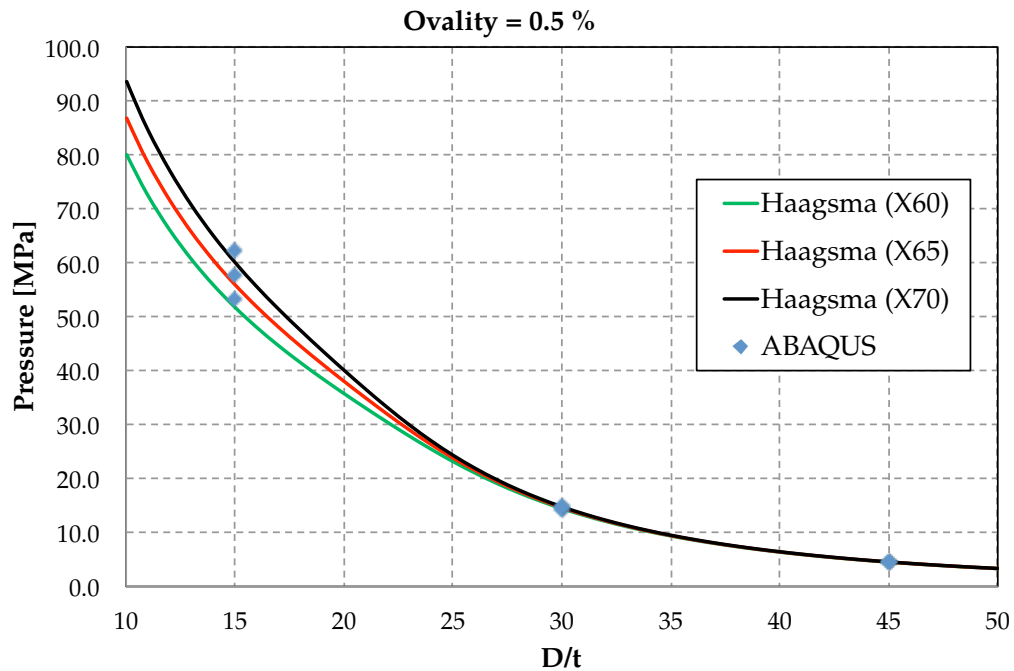
FIGURE 4.12: Result variation for diameter over thickness ratio. P_c is the collapse capasity from ABAQUS and P_0 is collapse capasity from *Haagsma* equation. The values are all with ovality of 0.5 %
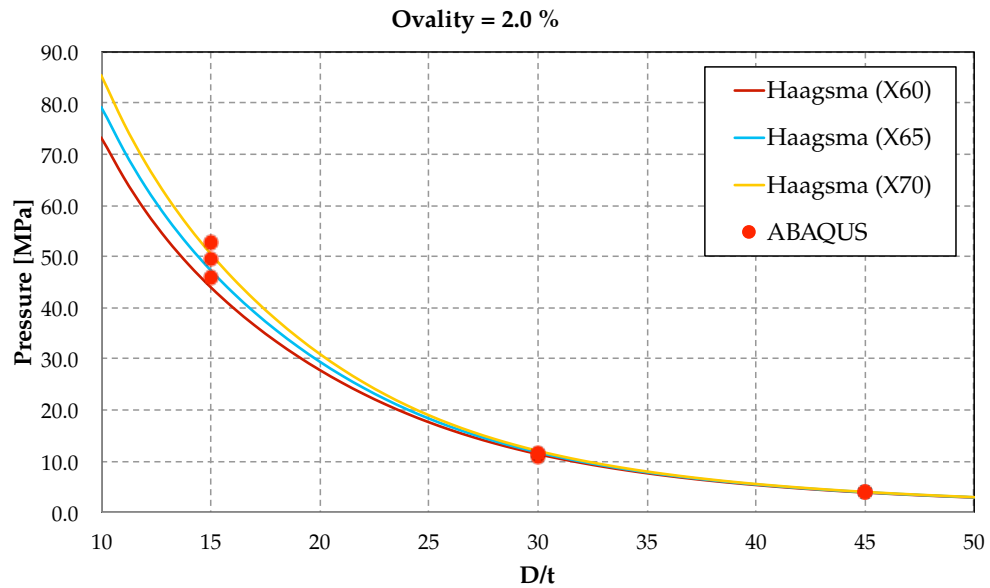
FIGURE 4.13: Result variation for diameter over thickness ratio. P_c is the collapse capasity from ABAQUS and P_0 is collapse capasity from *Haagsma* equation. The values are all with ovality of 2.0 %
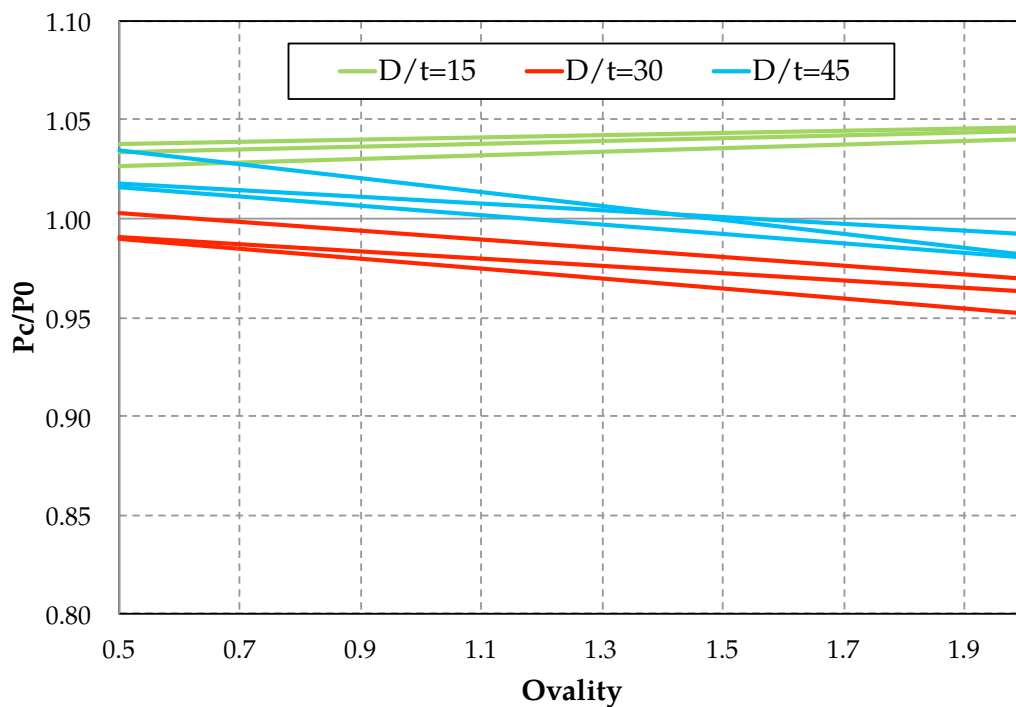
FIGURE 4.14: Collapse predictions vs. ABAQUS collapse values. Each colour group $\left(\frac{D}{t}\right)$ was tested with three steel materials.
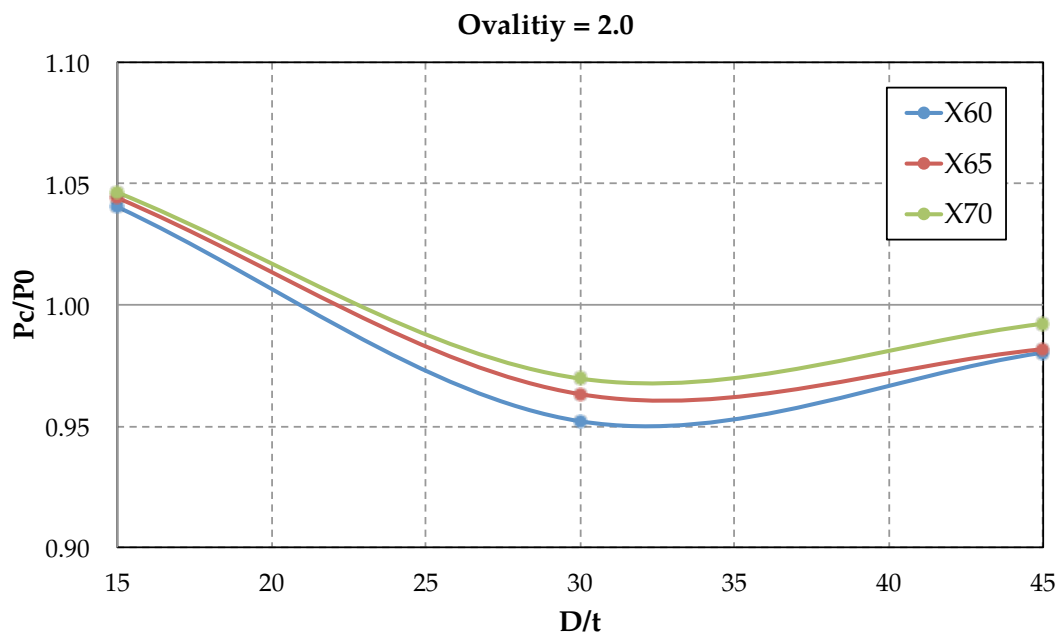
FIGURE 4.15: Collapse predictions vs. ABAQUS collapse values with respect to material quality. The plot is for pipes with ovality of 2.0 %.
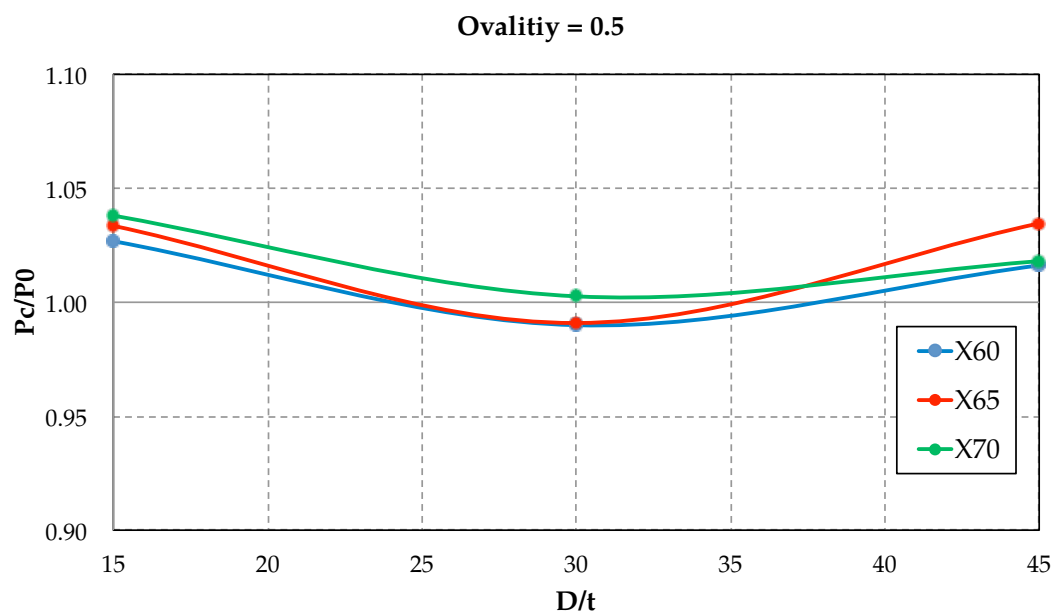
FIGURE 4.16: Collapse predictions vs. ABAQUS collapse values with respect to material quality. The plot is for pipes with ovality of 0.5 %.

4.4.3 Critical Diameter to Thickness Ratio.

In Chapter(2) a critical area in collapse pressure with $\frac{D}{t}$ ranging from 20-25 was discussed as the point where the predicted collapse capacity has its highest value deviated from its zero ovality path. In order to both compare this theory to our FE-model five specimens with $\frac{D}{t}$ of 10, 15, 20, 25 and 45 was simulated with ovality of 0.5 % and 1 %. Equally like the analytical calculation the ABAQUS collapse pressures where evaluated with Equation(2.10) and plotted in Figure(4.17).

Both curves paths seem to fit up to $\frac{D}{t}$ of 20, where ABAQUS shows larger distance from the zero ovality path all the way to $\frac{D}{t}$ of 45. I.e for both analytical calculation and ABAQUS simulations, the values of the predicted collapse capacity versus the *elastic* collapse capacity diverges. This is also clearly visible in Figure(2.4). Most importantly it it evident from Figure(4.17) that the critical $\frac{D}{t}$ is 25.
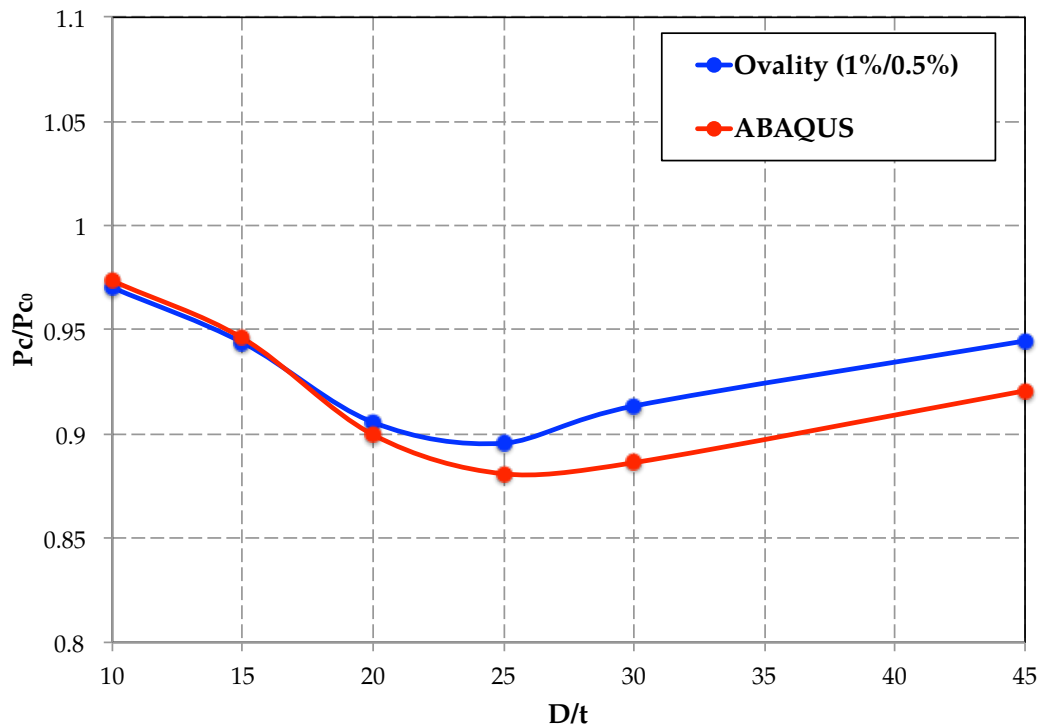
FIGURE 4.17: Critical diameter to thickness ratio verification. Shows the same as analytical formulation with highest value for $\frac{D}{t}$ of 25.

Chapter 5

FE- model With Coating

5.1 Introduction

This chapter describes the continuation of building the FE-model and implementation of coating. The results extracted from the uncoated model and presented at the end of last chapter has given a very accurate values for collapse capacity comparing with the *Haagsma* equation. Hence the goal in this part has been to minimise the geometry change and thus keeping the uncertainties constant when adding coating to the model. Furthermore the changes to the model are discussed followed by the case study of 12 different coating thicknesses.

5.2 Coating Implementation

The following subchapters describes the changes made to the FE-model to include both steel and coating material property and mesh criteria.

5.2.1 Coating Geometry

The FE- model that was built and described i Chapter(4) is not much unlike the coated model. The difference of the two is a partition of the cross section shown in Fig(5.3) at a desired thickness. In this way there would be no concern regarding contact surfaces (node connectivity, friction etc) as the pipe section behaves as one single body but

with two different material property definition. It is noted the assumption of zero slip condition between steel and coating before and at the moment of collapse. The boundary conditions where unchanged as the pipe section again stayed as one single body.

5.2.2 Material Data

Mainly there are two types of polymers used in multi layer coatings, polymer solid and foam as seen in the example in Table(5.2). Material stress-strain relationship is found for both material types in literature [18], [19] and [20]. The theory of stress-strain response accounting for temperature and strain rate for polymer solid with the following equations are presented from [18]:

The total strain assumed to have an elastic and a plastic part at any given stress:

$$\epsilon = \epsilon_e + \epsilon_p \tag{5.1}$$

The ϵ_e is the elastic and ϵ_p is the plastic strain. The elastic strain is defined as:

$$\epsilon_e = \frac{\sigma}{E(\dot{\epsilon}, T)} \tag{5.2}$$

where, E is the elastic modulus and is a function of strain rate $\dot{\epsilon}$, and temperature T. The plastic strain is assumed to be a function of stress and strain:

$$\epsilon_p = \beta(\sigma_y, \epsilon_y)\sigma\epsilon^m \tag{5.3}$$

Where β is a function of yield value of stress and strain. The m is strain exponent and describes the polymers strain hardening (m < 1) or softening (m > 1) behaviour. Strain hardening/softening is usually an indicator of the materials ability to sustain further stresses during plastic deformation. Combining the three equations, Equation(5.1) transforms to Equation(5.4):

$$\sigma = \frac{E(\dot{\epsilon}, T)\epsilon}{1 + E(\dot{\epsilon}, T)\beta(\sigma_y, \epsilon_y)\epsilon^m} \tag{5.4}$$

The strain rate and temperature dependent function of E [19] is expressed as:

$$E = E_0 \left(1 + m_1 \cdot ln\left(\frac{\dot{\epsilon}}{\dot{\epsilon_0}}\right)\right)^{-\lambda_1(T-T_0)} \tag{5.5}$$

Where m_1 and λ_1 are defined as strain rate strengthening coefficient and thermal softening coefficient respectively and they are material specific. The subscript $_0$ states the reference value. For strain softening material, β and strain exponent (m) can be expressed as:

$$m = \frac{E\epsilon_y}{E\epsilon_y - \sigma_y} \tag{5.6}$$

$$\beta = \frac{1}{(m-1)E\epsilon_y{}^m} \tag{5.7}$$

Where σ_y and ϵ_y are yield stress and strain respectively.

From [20] a conservative but realistic stress-strain relationship is presented for polypropylene foam. The stress-strain relationship gives a good fit up to about 8-10 % strain which is believed to be within the collapse strain.

$$\sigma = \frac{\sqrt{2}}{1000} \cdot E \left(\frac{1000n\epsilon}{\sqrt{2}} - n - 1\right)^{\frac{1}{n}} \tag{5.8}$$

Where n is a variable co-efficient witch is a function of strain:

$$n = 1 + 5\pi\epsilon \tag{5.9}$$

It is noted that the above formula is valid only for unit of pound per square inch (Psi). Also noted that Equation(5.8) is a function of elasticity of the material and the strain, but Equation(5.4) is dependent of strain rate $(\dot{\epsilon})$, temperature (T), yield strain (ϵ_y) and yield stress (σ_y) on top of elasticity and the strain. Figure(5.1) and (5.2) is plots of Equation(5.4) for values of elasticity found in [19]. The variation of elasticity is due to strain rate and temperature change. The values of plots in Figure(5.1) and (5.2) are given in Table(5.1).

TABLE 5.1: Polypropylene mechanical properties. The values are found from experimental data [19].

E- modulus	σ_y	ϵ_y
1610 $[MPa]$	35 $[MPa]$	13 %
760 $[MPa]$	25 $[MPa]$	16 %
440 $[MPa]$	18 $[MPa]$	18 %
250 $[MPa]$	14 $[MPa]$	18 %
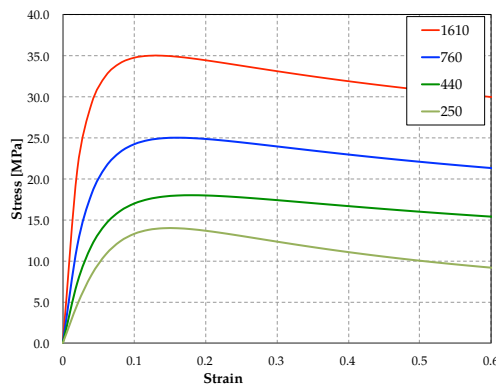
FIGURE 5.1: Engineering stress-strain curve for polypropylene with the values from Table(5.1) evalueted with Equation(5.4)
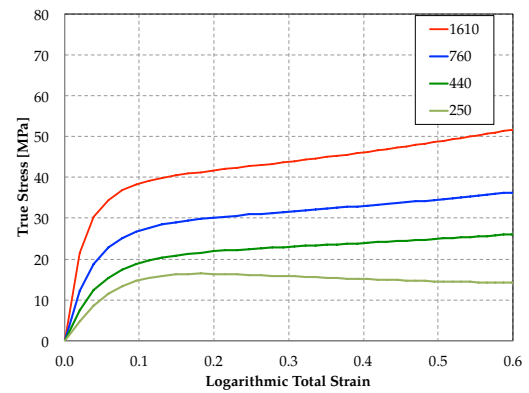
FIGURE 5.2: True stress and logarithmic strain curve for polypropylene from Figure(5.1) transformed with Equation(4.6).

TABLE 5.2: 7 layer polypropylene coating (7LPP) from the BP Thunderhorse Project [8].

Layer	Type	Description	Thickness
1	EP-F 2004	Epoxy	300 μm
2	BB127E	Adhesive	300 μm
3	BB108E-1199	Solid PP	8.4 mm
4	BB202E	Solid PP	30-40 mm
5	BB202E	PP Shield	4-5 mm
6	BA212E+ TR0103PP+ WB130HMS	PP Foam	25-43 mm
7	BA202E	PP Shield	5 mm

5.2.3 Mesh

In general meshing a FE-body one has to investigate where on the part it would be large stress and hence deformation gradients. At those areas one can define a more coarse mesh. Looking the now included coating material there would be no need to have the same mesh criteria as the steel part. The coating material with a much lower elasticity module than the steel would not be as affected to stress in any way as the steel part will. This is clearly illustrated in Figure(3.5) and (3.6).

Therefore the the coating mesh has not been tested for convergence hence only set for two elements per 100 mm of coating thickness seen in Figure(5.4)
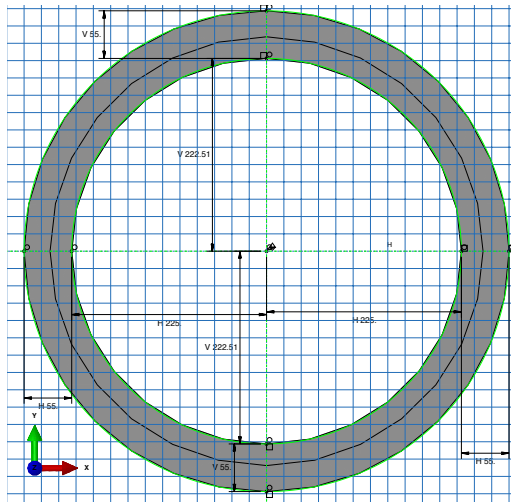
FIGURE 5.3: Illustration of the patitioned body in ABAQUS.
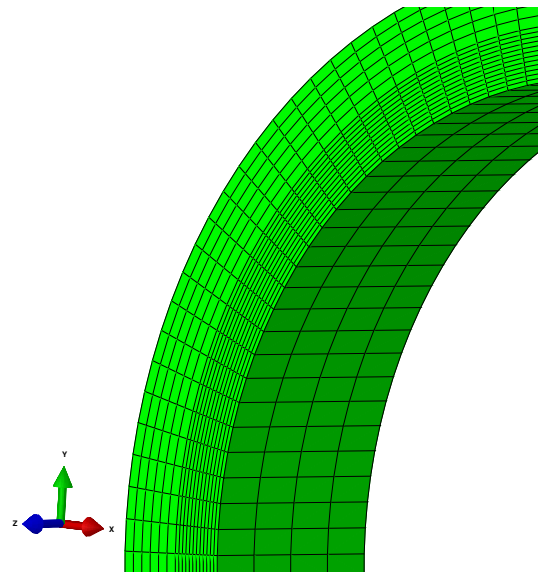
FIGURE 5.4: Mesh configuration for 30 mm. coating. The mesh configuration for the coated part where two elements pr 10 mm. thickness.

5.2.4 Coating Ovality

In the same manner as the coating is neglected in pipeline design there is not any known standards for coating measurements of ovality. Coating (polymer) is either melted and extruded in to a film and then layered on the pipe (large diameters) or extruded directly on to the pipe (small and medium diameters). In both applications the possibility of out-of-roundness is very much present. Not only with respect to production but also in regards to handling/storing a coated pipeline, ovality and other

imperfections may occur. Assuming ovality in coating is present one can wonder how the ovality is rotated comparing with the ovalliesed steel pipe as shown in Figure(5.9)
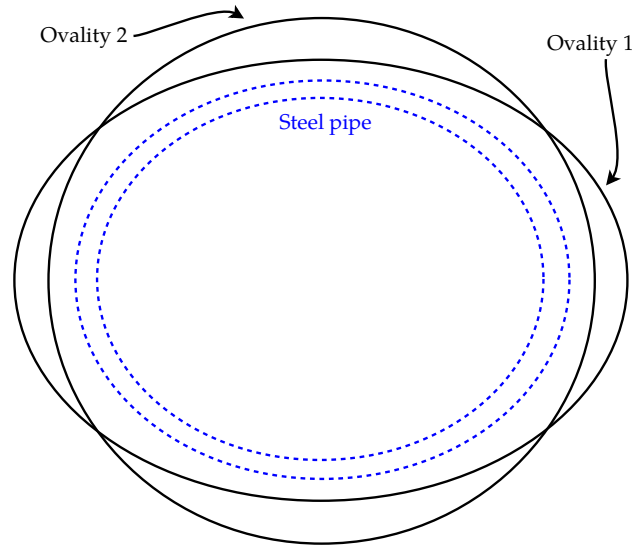
FIGURE 5.5: Coating ovality with two different orientation.

The assumed ovality of the coating is set to be similar to *Ovality 1* in Figure(5.9) for the case study in this thesis, and hence D_{max} and D_{min} of the coating will be parallel to D_{max} and D_{min} of the steel.

5.3 Sensitivity Study

For any non linear finite element analysis the results are only as good as the material model/properties input, hence one should be prudent when using the result from FE analysis. The material response of polymer to stress/strain are very different than steel behaviour and hence depending on the type of analysis, modelling thermoplastics as steel could give inaccurate results [21], [22].

Adding coating to the model has undoubtably added a variety of parameter that can be analysed. Those parameters can be number of layers with coating, different material property for each layer, different thickness for each layer etc. Already for

those three parameters mentioned one can make hundreds if not thousands of analysis. Hence for each added properties there must be added uncertainty involved. There has to be noted the change in material properties for polymers (that are mostly used for coating) with respect to strain rate and temperature. I.e. an polymer may behave like a glass at low temperatures, a rubbery solid at intermediate temperatures and more like viscous liquid if the temperature is raised further [14].

The material properties of Polypropylene solid and foam present in Chapter(5.2.2) are believed to be a good representation of the material used for the application at hand. As seen in Figure(5.1) and (5.2) the material softens after yield limit. This material behaviour is difficult to represent with only one material model, and hence two or several parallel models has to be used. A very suitable model is the Parallel Network Model (PNM) from *PolyUMod* library developed by *Jörgen Bergström*. This model solver with linking to ABAQUS is however licensed software and hence a trial version was acquired to do the analysis. For this approach it is noted that the enhanced hourglass stiffness must be applied for chosen elements in ABAQUS.

Normally in all engineering works and problem solving, the engineer will try to find the simplest way of representing the problem and hence save time and money by doing so. This statement is specially not excluding FE-simulations. With respect to our FE-model and the purpose of this thesis a simple but also accurate material model is needed for all coating thicknesses.

Thus a elastic-perfectly plastic and elastic with bilinear hardening approach has also been considered for a sensitivity study. As assumed in Chapter(3.3) the coating material plastic behaviour is believed to be not relevant for the case of collapse as the stress and strain will be in the linear area. This theory was set to be tested where seven materials with different hardening was simulated for a pipe with $\frac{D}{t}$ of 20 and a coating thickness ranging from 10 to 120 mm. The ovality was set to 1% for both the steel and the coating. The materials used is listed in Table(5.3) and plotted in Figure(5.6) and (5.7). The hardening modulus H witch is related the angel of the hardening line ($tan^{-1}(H)$) for the bilinear hardening models (Material 1-4) is defined as:

$$H = \frac{\sigma_u - \sigma_y}{\epsilon_u - \epsilon_y} \tag{5.10}$$

TABLE 5.3: Material properties for the sensivity test.

Material	E [MPa]	σ_y [MPa]	ϵ_y %	σ_u [MPa]	ϵ_u %	H
Hardning 1	1000	20	2 %	21	100	0.01
Hardning 2	1000	20	2 %	50	100	0.31
Hardning 3	1000	20	2 %	100	100	0.82
Hardning 4	1000	20	2 %	150	100	1.33
PP-ISO	1000	20	8 %	21	100	0.01
PP-PNM	1000	20	8 %			
PP-FOAM	1000	15	4 %			
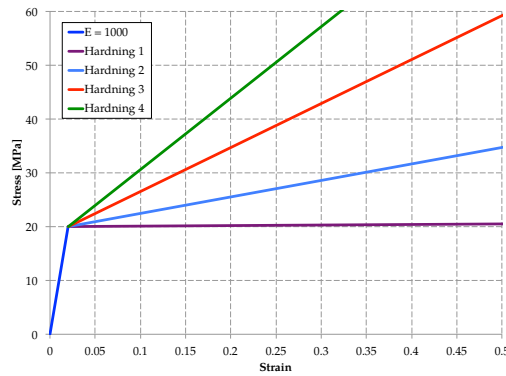
FIGURE 5.6: Sensitivity study materials. *E* is 1000 [MPa], yield stress is 20[MPa] and ultimate stress is set for 21, 50 ,100 and 150 [MPa] for *Hardining* 1, 2, 3 and 4 respectively with ultimate strain of 100%.
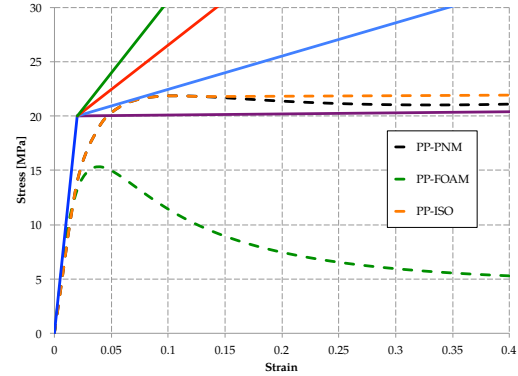
FIGURE 5.7: PP-PNM (polypropylene-Parallel Network Model) from Equation(5.4), PP-FOAM (Parallel Network Model)) is a plot of Equation(5.8) and PP-ISO is a combination material with metal plasticity up to the yield point and perfectly plastic after. PP-ISO has the same values of E, σ_y and ϵ_y as PP-PNM.
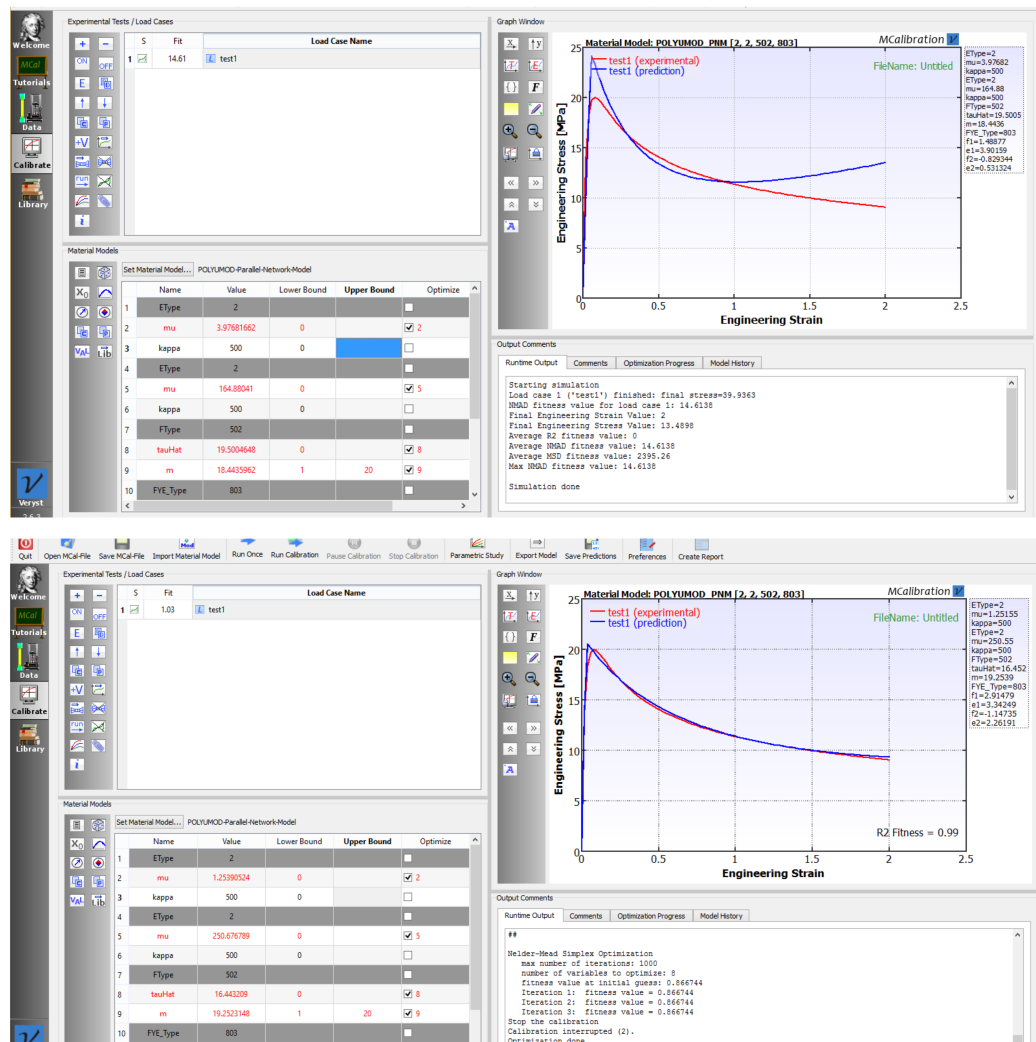
FIGURE 5.8: Calibration of material model of Parallel Network Model (PNM) with *Mcalibration*. The figures shows the calibration of the PP-FOAM material for the sensivity study. Top figure shows the first calibration run and bottom figure shows the calibrated model. As can bee seen from the calibrated model, the curve is perfectly fitted (R2 Fitness=99%).

5.3.1 Sensitivity Results

Running all 12 pipe sections with the coating materials listed in Table(5.3) the result shows at the most 0.06% change in the collapse resistance for material with hardening 1-4. That is considered as no change in FE- analysis and hence there was no stress level in the coating above yield point. For the PP-ISO the collapse capacity followed the the mentioned materials perfectly up to 60 mm coating and then flattening out to lower values up to 120 mm. For the PP-PNM and PP-FOAM witch was calibrated

with *MCalibration* and *PolUMod* software seen in Figure(5.8) have shown a rather conservative collapse pressure.

With the lack of experimental data for the application of collapse needed to verify the results one cannot conclude one material better than the other, however the calibrated materials is believed to be more correct that of those with metal plasticity. Even if the coating strain is low at the moment of collapse the material has to withstand the radial pressure of almost the double size of the yield stress and thus correct material model for high stress is preferred. With respect to the collapse results some remarks has been stated:

- Plastic hardening is not of importance as material with hardening 1-4 is showing the exact same collapse values. This statement is true for $\sigma_y = 20$ [MPa].

- The calibrated material models of PP-PNM is resulting in a surprisingly lower collapse capacity then PP-ISO that arises from the same equation.

- The metal plasticity (PP-ISO) is not a suitable material model for this analysis as it does not account for the viscoelasticity of the material.

- The Parallel Network Model of *Jörgen Bergström* is the most conservative of the all the models tested and is believed to be the most accurate in terms of stress-strain response.

The conclusion of the sensitive study is that elastic perfectly plastic material models and also metal plasticity would be suitable for thin and medium thick (< 60 mm) coatings but are not accurate for thick (> 60 mm) coatings simulations. Hence the goal of finding a simple material model for simulation of thin and thick coating has not succeeded. Hence the PNM material model will be considered for the case study.
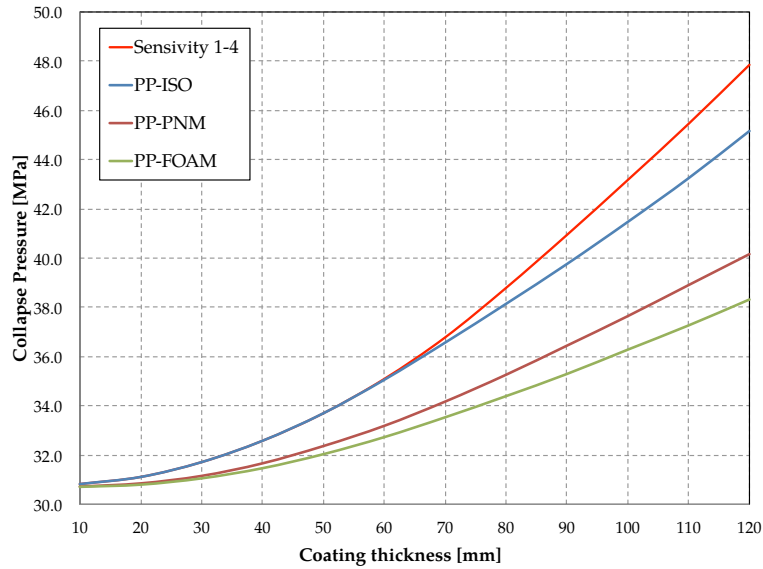
FIGURE 5.9: Results of sensivity study.

5.4 Case Study

A case study is proposed to investigate the collapse resistance when altering the coating parameters.

5.4.1 Preliminaries

For any finite element simulation, solvers request input values of boundary & loads, geometrical and material data from the user. In order to studying the problem in a range of parameters the mentioned values can be varied. For the criteria stated above the uncoated model has shown to be very accurate in comparison to analytical formulation. Developing the model further it has simply only been added one extra material definition(coating). From the sensitivity study the results has shown that the coating stress levels was below the yield points and only increased the pipe collapse limit. Thus it has been appropriate to investigate the collapse effect of Polypropylene foam witch is softer material and has much lower yield limit.

Considering the vast amount of parameters that can be included in such study it has been necessary to make certain assumptions. Coating material model from Equation(5.8) was calibrated with *MCalibration* software with varying Young's modulus . For the geometrical parameters of the steel only $\frac{D}{t}$ of 20 and ovality of 1.0 % was studied. For the coating part three ovality values was investigated. For all models only one coating layer has been considered with thickness variation from 10 to 120 mm. The analysis was preformed with the purpose of testing the steel pipe with all possible parameter configuration, hence changing one parameter value all other was kept constant. This approach resulted in 144 test runs in ABAQUS. The parameters included in this study is listed in Table(5.4).

TABLE 5.4: Case study geometrical and material parameters with start and stop and increment values.

Parameter	Values start	Value stop	Increment
Coating Ovality	0.5%	1.5%	0.5%
Coating thickness	10	120 mm	10 mm
Elasticity	250 [MPa]	1000 [MPa]	250 [MPa]

5.4.2 Effects of Coating Thickness

The results of collapse capacity of the pipe with respect to coating thickness is mostly as expected. The values are presented as:

$$Results = \frac{P_c}{P_0} \tag{5.11}$$

Where P_c and P_0 is the collapse pressure with and without coating respectively.

From Figure(5.10) it is evident that the collapse limit increases as the coating thickness increases. However thickness up to approximate 30 mm shows a decrease in the collapse capacity and from Figure(5.11) it is clear that increasing the elastic stiffness of the material will decrease the collapse capacity. The decrease values are not greater that 0.7 % but it is nevertheless interesting findings. The increase in collapse capacity

is seen to be between 5 and 25 % on the thickest (120 mm) layer.

In Figure(5.12) the theory of serial resistance from Chapter(3.3.2) is compared to the ABAQUS results. For both models the elasticity of 1000 MPa was evaluated and the results are very promising for coating thickness up to 70 mm witch is a fairly large amount of coating. For the thickest coating the serial resistance theory predicts 15 % increase to 25 % of ABAQUS. Overall this simple theory has shown to be a very easy and simple calculation method for collapse capacity prediction of coated pipelines.
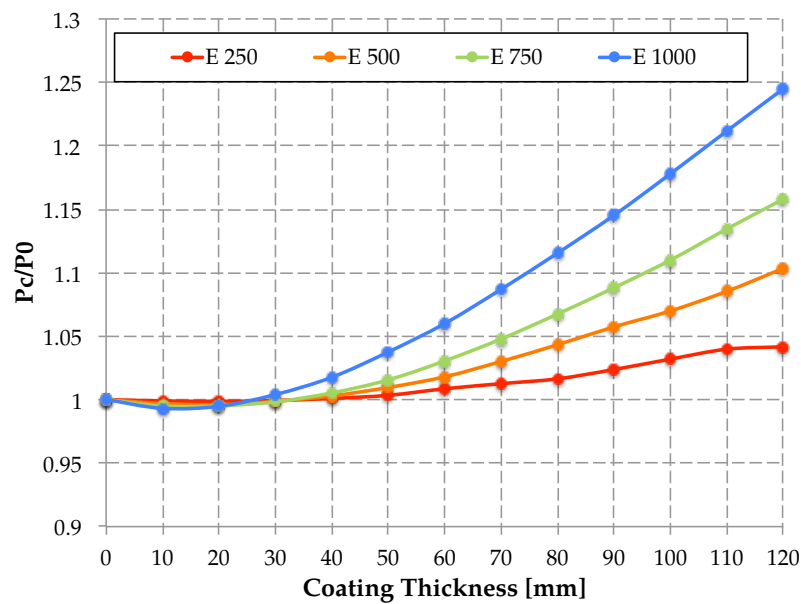
FIGURE 5.10: Collapse capacity vs coating thickness for elasticity of 250, 500, 750 and 1000 MPa
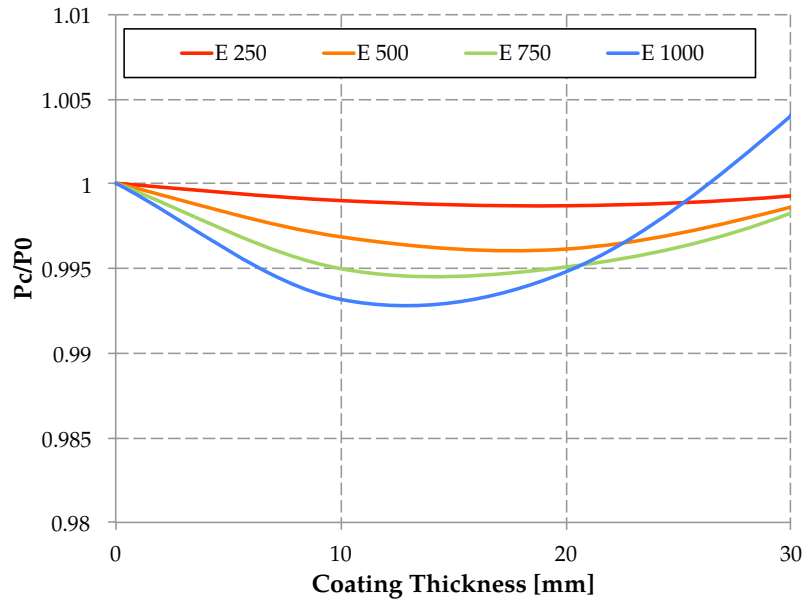
FIGURE 5.11: Enlarged area with negative effect.
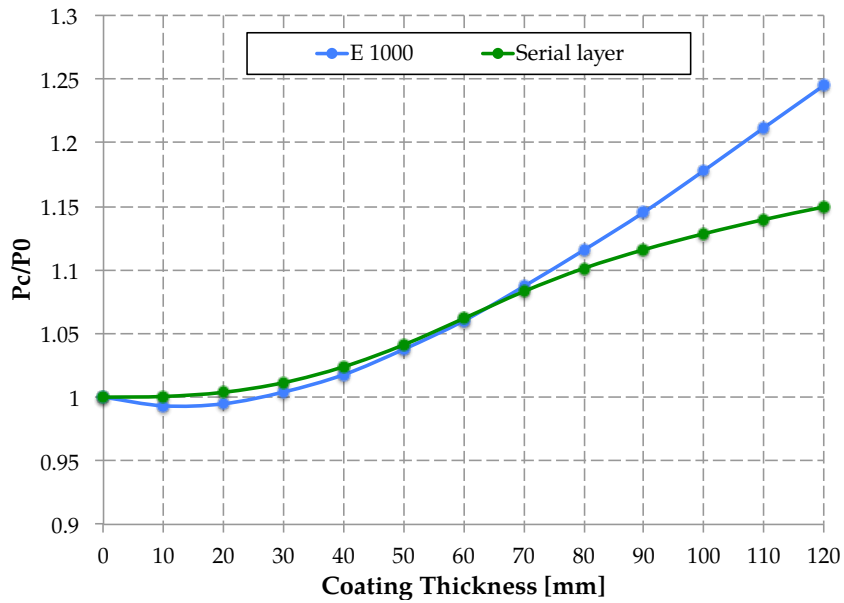
FIGURE 5.12: The theory of serial resistance collapse capacity in comparison with PNM of 1000 MPa.

5.4.3 Effects of Coating Ovality

The analysis of ovality variation has shown not to effect the collapse capacity in any significant way. The lines in Figure(5.13) are almost strait lines and moving from

0.5% to 1.5% yield almost no visible effects. Hence one can not expect any significant change to the collapse capacity even with the influence of much larger out of roundness values.
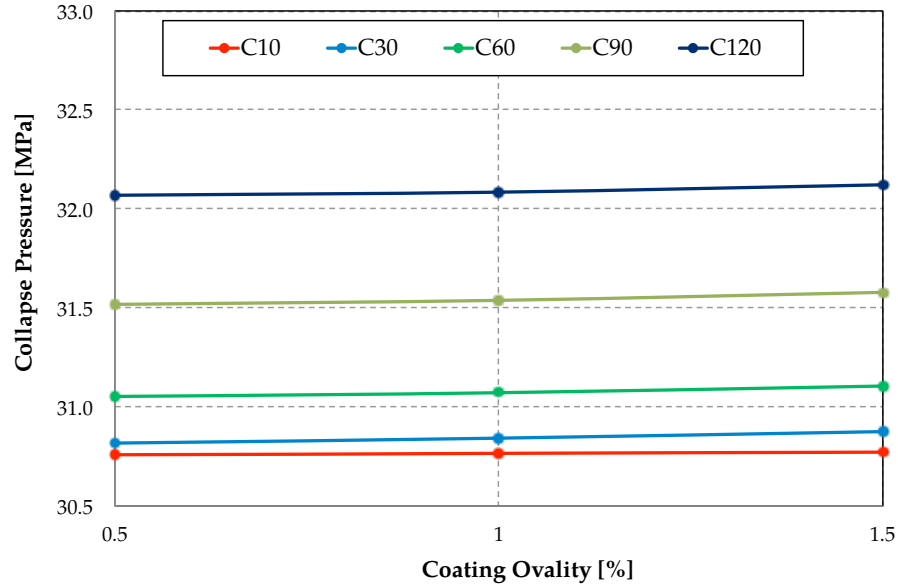
FIGURE 5.13: Collapse capacity vs coating ovality.

5.4.4 Effects of Coating Elasticity

The effects of elasticity is not surprisingly much different than effects of coating thickness. Increasing the elasticity will increase the collapse resistance. As the material surrounding the steel pipe get stronger or stiffer the pipe ability to withstand the outer pressure increases. The value of 250 MPa is wisely chosen for the parameter study as according to [20] it is representative of the true elasticity of the overall coating strength, even as the elasticity of Polypropylene solid is higher. Hence varying the elasticity up to 1000 MPa is believed to correct for any variation of material layers with respect to solid and foam.

The results of elasticity from the analysis is presented in Figure(5.14) and (5.15). It is clearly visible the decline of collapse capacity for coating layer 10 mm and 20 mm as the elasticity increases.
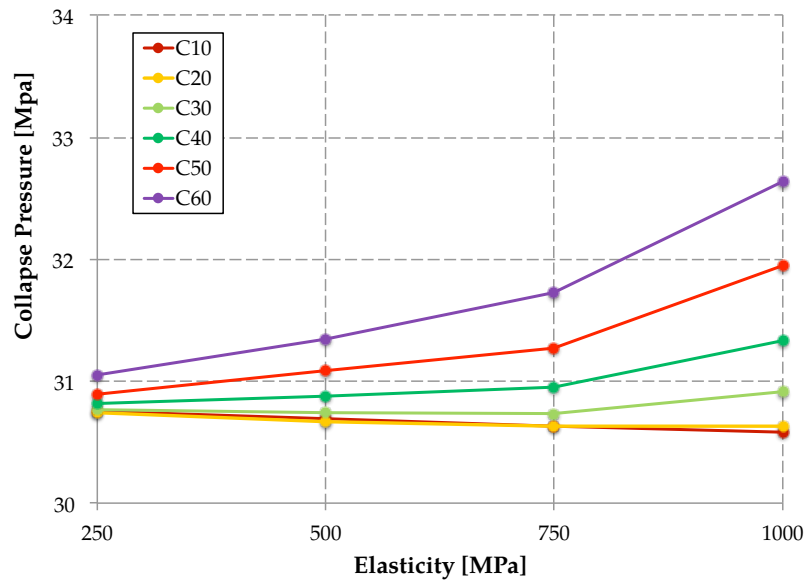
FIGURE 5.14: Collapse capacity vs elasticity for coating thickness 10-60 mm.
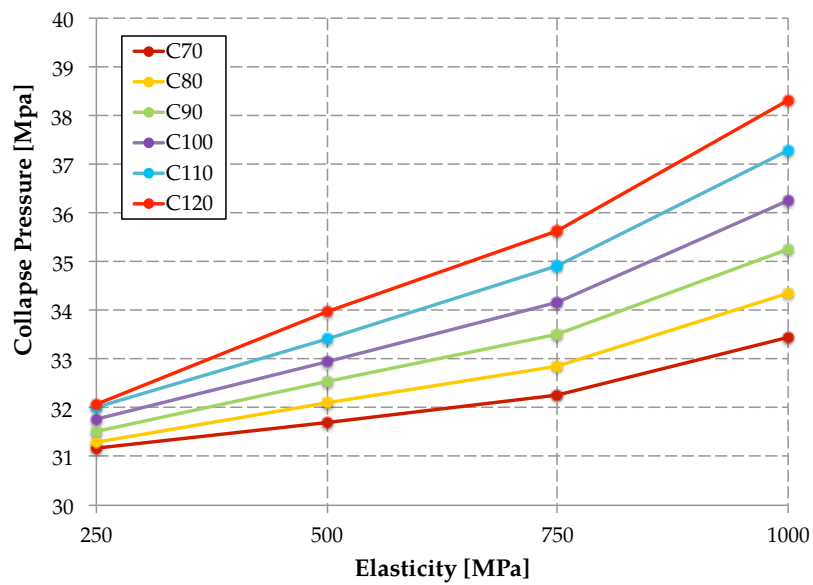
FIGURE 5.15: Collapse capacity vs elasticity for coating thickness 70-120 mm.

Chapter 6

Discussion and Conclusions

6.1 Discussion of Results

In summary the result of this project has been at first the collapse capacity of a uncoated pipe section in ABAQUS and the verification of the results to *Haagsma* collapse equation. Further on the geometrically unaltered ABAQUS model has been simulated with coating in order to see the effects with respect to the collapse capacity.

The uncoated model has shown a very accurate prediction of the collapse capacity in comparison to the *Haagsma* and thereby the DNV-OS-F101 collapse equation. The ABAQUS results where within 5 % of the DNV model and hence it is believed to be a very good finite element model.

Recent study done on pipeline collapse including FE- analysis has shown similar result. A study done by [23], the collapse of imperfect subsea pipelines was evaluated with numerical (FE), analytical and experimental approach. The analytical solution was derived mathematically. The results from analytical collapse pressure vs. FE-analysis also diverges approximately 5%. The comparison pipe specimens are listed in Table(6.1).

TABLE 6.1: Comparison of test results for [23]. Subscripts of $_{ex}$, $_{th}$ and $_{FA}$ are experiments, theory and FA-analysis respectively. The error is $P_{FA} \cdot 100 / P_{th}$. The analysis was done with steel quality of X65

D/t	f_0 %	P_{ex} [MPa]	P_{th} [MPa]	P_{FA} [MPa]	error %
32.50	0.54	10.16	10.53	10.55	0.2
40.60	0.32	5.22	5.56	5.85	5.2
54.20	0.46	1.87	2.02	1.96	3.0

A study done by [24] on asymmetric collapse of offshore pipelines also developed a mathematical expression for collapse prediction. Comparison of the results to ABAQUS values had less difference than 5 %. The theoretical model was developed for predicting the collapse pressure of a tube with arbitrary initial geometric imperfections. In this article no exact values for imperfections was given and the following presented values of ovality are approximate based on graphs. The values in Table(6.2) is taken from the parametric study in [24].

TABLE 6.2: Comparison of test results for [24]. Subscripts of $_{th}$ and $_{FA}$ are theory and FA-analysis respectively. The error is $P_{FA} \cdot 100 / P_{th}$. The analysis was done with steel quality of X65.

D/t	f_0 %	P_{th} [MPa]	P_{FA} [MPa]	error %
20	0.33	37.40	35.80	4.3

A very comparable study done by [25], where the ultra-deepwater pipelines collapse analysis was conducted including ANSYS FE-solver and the *Haagsma* and thereby the DNV-OS-F101 collapse equation. The values presented in Table(6.3) shows a error from less than 1 % to 10.7 % with the same analytical model used in this thesis. Showing that another FE-program produces similar collapse data it is evident that the values presented from our uncoated model is reasonable and reliable.

TABLE 6.3: Comparison of test results for [23]. Subscripts of $_{th}$ and $_{FA}$ are theory and FA-analysis respectively. The error is $P_{FA} \cdot 100/P_{th}$. The analysis was done with steel quality of X65.

D/t	f_0 %	P_{th} [MPa]	P_{FA} [MPa]	error %
9.86	1.00	86.1	87.0	1.0
11.50	1.00	72.6	71.9	0.9
15.35	1.00	51.3	48.5	5.5
19.68	1.00	35.5	32.0	9.9
25.07	1.00	21.4	19.1	10.7

Producing a geometrical element model, defining a good mesh and material model for such a simple collapse problem in separate is not however "fine art". But doing them all together perfectly and understanding the data is. This model was made for the purpose of quality assurance as the analytical models available today has shown to be accurate and appropriate for comparison. The goal has been to minimise the uncertainties related to boundary condition, meshing etc. when the FE-model was developed further with the influence of coating. This approach has been successful as the uncoated pipe left no room for questioning the quality of the collapse data and hence the FE-model.

Moving on with the coated model most of the effort was left defining an appropriate material model for the coating section. This is where most of the uncertainties exist as polymer material are more complex and in many ways different than steel in behaviour, also no data was found for comparison purposes for this particular problem. However a large amount of research has been conducted on sandwich pipe for deepwater applications, witch to some extent contains collapse relevant data.

In this text the contact surface between the steel and the coating was considered to be of perfect adhesion where the nodes are shared along the interface. In [26] the same approach has been used for the same reason of simplicity. The topic of perfect adhesion vs no adhesion is also the subject of numerous studies. In [27] the perfect adhesion option showed a overestimation of the collapse pressure while the no adhesion version

approximated the collapse data. In addition a better correlation between numerical and experimental data was obtained when added friction was introduced between the layers. Also in [28] the no adhesion and perfect adhesion bonding was studied where the latter showed a higher collapse pressure, however without any experimental data for comparison. In[29] comparison between the two adhesion bondings has shown mostly good relation to experimental data. It is noted that for the mentioned studies the pipes are of sandwich pipes with two metallic layers where the angular space are filled with insulating material. The inner metallic pipe and the insulating material is normally produced in the same manner as the coated pipes investigated in this thesis, i.e with extrusion. Thus there is reason to believe the adhesion of the outer metallic pipe with the outer area of the insulating material is not as strong as the first layer as the fitting is made of the two sections pressed on to each other and epoxied. Hence the less adhesive bonding between the second and third layer may reduce the overall stiffness of the pipe resulting in lower collapse capacity

Thus based on the difference geometry of sandwich pipes and single layer coating, it is believed that the choice of perfect adhesion has given reasonable results in this thesis.

Based on available research on polymer modelling and coating, a suitable material model with stress-strain relationship given in Equation(5.8) was calibrated with *MCalibration* software. The choice with values of elasticity ranging from 250-1000 MPa is meant to account for a average elasticity of all layers of coating. Also the difference thickness in coating layers from different, manufacturers or subsea project will result in an average elasticity variation. The simulated, coated pipeline has given collapse data indicating the increase of the collapse capacity when the coating thickness increases. The increase in the collapse capacity is shown to be related to the increase of the pipeline stiffness but not affected of the coating out of roundness. In [27] metallic pipe with composite coating was studied with the aim of testing the composite material in conjunction with the metal pipe under external pressure. The results showed a significant increase in the collapse capacity. In Table(6.4) the results from [27] is listed.

TABLE 6.4: Concluding results for [27]. t_c and t is the coating thickness and steel thickness respectively. P_c and P_0 is the collapse pressure with and without coating respectively.

D/t	t_c/t	P_c/P_0
35	2	5.00
35	3	7.50
25	3	9.09

There is noted the large increase in collapse capacity of Table(6.4) compared to the result of this thesis is due to the large difference of stiffness in the composite material. For coating thickness from 0 to 25 mm. the collapse capacity has shown to decrease when increasing the material elasticity. However the decrease is not more than 0.7 % and thus not found be of significance. Also the latter results could be a consequence of numerical error.

6.2 Conclusions

In this project the collapse capacity of submarine pipelines with coating is studied. The collapse of steel pipe and of general collapse phenomenon is widely researched and it is evident that the subject is a complex issue involving many parameters and uncertainties. The *Haagsma* equation is used in DNV-OS-F101 pipeline standard and its believed to be the best model for prediction of pipeline collapse.

In the first part of this thesis two theories of pipeline collapse prediction with the effect of coating was discussed. The first theory was rather an indication of earlier collapse compared to bare steel pipe when stating the increase of the compressive hoop stress of a coated pipe when subjected to external pressure. This statement was not accounting for the coating stiffness. The second theory was stating the opposite saying the collapse resistance of a coated steel pipe is increased as the collapse resistance of a bare steel pipe is to be added to the collapse resistance of a bare coated pipe. This statement is essentially saying; If the coating is stiff enough to hold its own weight

an not collapse in atmospheric pressure, it will then resist some of the water pressure when submerged and added on to a steel pipe increasing the overall collapse resistance.

In the first part of the analysis, the collapse of a uncoated pipe section was studied in order to verify the FE-model. Firstly a mesh convergence test was done to find the best configuration of elements in both radial and circumferential direction. The best configuration with respect to computational time and collapse results was found to be 12 and 30 elements in thickness and circumferential direction respectively. The circumferential number of elements is referred to as elements per quarter pipe, hence for the hole pipe we get 120 elements. The collapse data was compared to the *Haagsma* collapse equation and the result showed a deviation not larger than 5 %. For pipes with high $\frac{D}{t}$ (thin pipes) the results deviated less than for pipes with lower (thick pipes) $\frac{D}{t}$. The latter part of the uncoated pipe analysis a critical $\frac{D}{t}$ of 25 was found indicating the point where the predicted collapse will deviate mostly from its zero ovality path. This finding was also compared to analytical data where the results matched.

Moving on to the coated pipe section and the objective of this thesis, analysis has shown that the coating will increase the collapse capacity as added thickness increases. The material elasticity of the coating and thereby the stiffness of the coated part is the key to whether the collapse capacity increases or not. Increasing coating stiffness will result in higher collapse resistance. The results from the sensitivity study performed with different coating material models has shown the collapse strain is in the elastic area at the point of collapse and not affected by any hardening modulus. The parameter study that was preformed with material models calibrated by *MCalibration* and *PolyUmod* library software connected with ABAQUS has shown a increase of collapse resistance for all elasticity models ranging from 250-1000 MPa. At the highest thickness the increase was seen between 5 and 25 %. Also the results has shown that coating ovality does not affect the collapse capacity in any significant way.

Looking back the latter theory mentioned in this chapter has shown to predict the increase of collapse capacity accurately up to 70-80 mm. of coating. For the thickest coating of 120 mm. the increase of collapse resistance was calculated to 15 % to ABAQUS 25%. Thus the author recommends the use of this simple calculation method for future calculation of collapse resistance for isotropic coating material. For

future work a study is proposed to investigate the possibilities of steel pipe thickness reduction when adding thick coating. Any reduction of steel thickness will presumably result in a massive cost reduction.

Bibliography

[1] Douglas-Westwood. Opportunities and outlook for the subsea sector. Subsea Australia Conference, 20th February 2013.

[2] DNV. *Submarine Pipeline Systems*. Den Norske Veritas, Høvik, august 2012 edition, 2012.

[3] S. Kyriakides and E. Corona. *Mechanics of Offshore Pipelines*, volume 1:Buckling and Collapse. Elseveier BV, 1 edition, 2007.

[4] Olav Aamlid, Leif Collberg, and Simon Slater. Collapse capcity of uoe deepwater linepipe. *Proceedings of the ASME 2011*, (OMAE2011-490), 2011.

[5] C.E Murphey and C.G. Langer. Ultimate pipe strength under bending, collapse and fatigue. *OMAE 1985*, pages 467–477, 1985.

[6] Erica Marley. Collapse capacity of submarine pipelines. Master's thesis, NTNU, 2011.

[7] DNV. *Pipeline Filed Joint Coating and Filed Repair of Linepipe Coating*. Den Norske Veritas, Høvik, may 2011 edition, May 2011.

[8] Shiwei William Guan, Nick Gritis, Adam Jackson, and Peter Singh. Advanced onshore and offshore pipeline coating technologies. China International Oil and Gas Pipeline Technology Conference and Expo, 14-17 September 2005.

[9] JFE Steel Corporation. Pipe coatings. Pipe and Tubes catalogs.

[10] Dr Shiwei William Guan. Subsea and deepwater flow assurance insulation. In Shawcor, editor, *Challenges and New Development*. Den Norske Veritas (DNV) Pipelines Open Day, November 2012.

[11] Rob Hunter. Wet insulation evolves to meet subsea flowline performance demands. In *Offshore*, chapter Transportation and Pipeline, page 2. Penn Well Corporation, october 2008 edition, 2008.

[12] Andrew C. Palmer and Roger A. Kings. *Subsea Pipeline Engineering*. Penn Well Corporation, 2nd edition edition, 2008.

[13] Bredero Shaw. Hevicote concrete weight coating. Product data sheet, January 2015.

[14] Callister William D. *Material Science and Engineering An Introduction*. John Wiley & Sons, Inc, 2007.

[15] Olav Fyrileiv and Leif Vollberg. Influence of pressure in pipeline design-effective axial force. *OMAE2005-67502*, June 12-17 2005.

[16] C.P Sparks. The influence of tension, pressure and weight on pipeand and riser deformations and stresses. *ASME transaction*, 106:46–54, 1984.

[17] Takaya Kobayashi and Yasuko Mihara. Application of abaqus for practical post-buckling analysis of cylindrical shells under axial compression. *Mechanical Design & Analysis Corporation*, 2010 SIMULIA Customer Conference 15.

[18] Yuanxin Zhou and K. Mallick. Effects of temperature and strain rate on the tessile behavior of unfilled and talc-filled polypropylene. *Part 2*, 42(12), Desember 2002.

[19] Yuanxin Zhou and K. Mallick. Effects of temperature and strain rate on the tessile behavior of unfilled and talc-filled polypropylene. *Part 1*, 42(12), Desember 2002.

[20] Gautam Chaudhury. Reeling of pipes with thick insulation, a simple new calculation procedure. *OTC 16111*, 2004.

[21] M Hovden. Tests and numerical simulations of polymer components. Master's thesis, Norges Teknisk-Naturvitenskapelige Universitet, NTNU, 2010.

[22] H Daiyan. *Experimantal and Numerical Investigation of the Mechanical Response of Injected Moulded Polypropylene*. PhD thesis, University of Oslo, UiO, 2011.

[23] Yu Jianxing, Li Zhibo, Yang Yuan, and Sun Zhenzhou. Collapse analysis of imperfect subsea piplines based on 2d high-order nonlinear model. *Transaction of Tianjin University*, 20(3):157–162, 2014.

[24] Shun feng Gong, Xing yue Ni, Sheng Bao, and Yong Bai. Asymmetric collapse of offshore piplines under external pressure. *Ships and Offshore Structures*, 8:2 (DOI:1080/17445302.2012.691273):176–188, 2012.

[25] Marco A. P. Rosas, Marco V. Rodrigues, Ana Paula F. Souza, and Danilo Machado L. da Silva. Hydrostatic collapse pressure and radial collapse force comparisons for ultra-deepwater piplines. *Proceedings of the ASME 2014*, Pipeline and Riser Technology(OMAE2014-24081):V06BT04A008.

[26] I.P. Pasqualino, B.C. Pinheiro, and S.F. Estefen. Comparative structural analysis between sandwich and steel pipelines for ultra-deep waters. *Proceedings of the OMAE 2002*, (OMAE2002-28455):165–173.

[27] S.C Oliveira Jr, I.P. Pasqualino, and T.A. Netto. Metal-compisite pipes for deepwater applications. *Proceedings of COBEM 2005*.

[28] B.C. Pinheiro, R.D. Ribeiro, and I.P. Pasqualino. Collapse pressure of damaged sandwich pipes. *Proceedings of COBEM 2007*.

[29] T.A. Netto, J.M.C. Santos, and S.F. Estefen. Sandwich pipes for ultra-deep waters. *Proceedings of IPC'02*, (IPC2002-27426), 2002.

Appendix A

Analytical Solutions

Haagsma Equation Solution

Haagsma equation:

$$(P_c - P_{el}) \cdot (P_c{}^2 - P_{pl}{}^2) = P_c P_{el} P_{pl} f_0 \frac{D}{t} \tag{A.1}$$

The solution of the *Haagsma* equation used in DNV-OS.F101 can be seen as a third polynomial where the unknown collapse pressure P_c is x in Equation(A.2):

$$ax^3 + bx^2 + cx + d = 0 \tag{A.2}$$

The solution is given as:

$$P_c = y - \frac{b}{3} \tag{A.3}$$

$$b = -P_{el} \tag{A.4}$$

$$y = -2\sqrt{-u} \cdot cos\left(\frac{\Phi}{3} + \frac{60\pi}{180}\right) \tag{A.5}$$

$$u = \frac{1}{3}\left(-\frac{1}{3}b^2 + c\right) \tag{A.6}$$

$$\Phi = arccos\left(\frac{-v}{\sqrt{-u^3}}\right) \tag{A.7}$$

$$v = \frac{1}{2}\left(-\frac{2b^3}{27} - \frac{bc}{3} + d\right) \tag{A.8}$$

$$c = P_{pl}{}^2 + P_{el}P_{pl}f_0\frac{D}{t} \tag{A.9}$$

$$d = P_{el}P_{pl}{}^2 \tag{A.10}$$

$$v = \frac{1}{2}\left(-\frac{2b^3}{27} - \frac{bc}{3} + d\right) \tag{A.11}$$

Appendix B

Results

B.1 Results of uncoated pipe in Abaqus.

TABLE B.1: Result of 18 pipe sections listed with ther geometry and property values. Collapse pressure(P_c) is calculated by LPF multiplied with external pressure (P_e).

Specimen	D/t	f_0	Material	LPF	P_e	P_c
1	15	0.5	X60	0.886282	60	53.17692
2	15	2.0	X60	0.763340	60	45.80040
3	15	0.5	X65	0.963631	60	57.81786
4	15	2.0	X65	0.822888	60	49.37328
5	15	0.5	X70	1.037920	60	62.27520
6	15	2.0	X70	0.879822	60	52.78932
7	30	0.5	X60	0.241615	60	14.29476
8	30	2.0	X60	0.187812	60	10.82388
9	30	0.5	X65	0.246974	60	14.49690
10	30	2.0	X65	0.187812	60	11.26872
11	30	0.5	X70	0.246974	60	14.81844
12	30	2.0	X70	0.193753	60	11.62518
13	45	0.5	X60	0.076553	60	4.593186
14	45	2.0	X60	0.062903	60	3.774150
15	45	0.5	X65	0.076735	60	4.604070
16	45	2.0	X65	0.064138	60	3.848274

TABLE B.1: *Continued*

17	45	0.5	X70	0.077372	60	4.642326
18	45	2.0	X70	0.065650	60	3.939006

B.2 Results of uncoated pipe in Abaqus in comparison with *Haagsma* equation.

TABLE B.2: FE result of 18 pipe sections in comaprison with the *Haagsma* equation. The variation is between 0 and less that 5 % shown in last column.

Specimen	D/t	f_0	Abaqus P_c [MPa]	Haagsma P_c [MPa]	$\frac{Abaqus}{Haagsma}$
1	15	0.5	53.17692	51.80	1.0266
2	15	2.0	45.80040	44.03	1.0402
3	15	0.5	57.81786	55.94	1.0336
4	15	2.0	49.37328	47.28	1.0443
5	15	0.5	62.27520	60.01	1.0377
6	15	2.0	52.78932	50.46	1.0462
7	30	0.5	14.29476	14.44	0.9899
8	30	2.0	10.82388	11.37	0.9520
9	30	0.5	14.49690	14.63	0.9909
10	30	2.0	11.26872	11.70	0.9631
11	30	0.5	14.81844	14.78	1.0026
12	30	2.0	11.62518	11.99	0.9696
13	45	0.5	4.593186	4.52	1.0162
14	45	2.0	3.774150	3.85	0.9803
15	45	0.5	4.604070	4.45	1.0346
16	45	2.0	3.848274	3.92	0.9817
17	45	0.5	4.642326	4.56	1.0181
18	45	2.0	3.939006	3.97	0.9922

B.3 Results of Sensitivity study.

TABLE B.3: Results of Mat_1 of the sensitivity study.

Thickness	LPF	P_c
10	30,82440	30,76626
20	31,11402	30,76536
30	31,71690	30,78828
40	32,58378	30,84288
50	33,70038	30,91944
60	35,09562	31,07232
70	36,78192	31,19760
80	38,79072	31,31574
90	40,94154	31,53870
100	43,17426	31,78644
110	45,45726	32,02476
120	47,85486	32,08500

TABLE B.4: Results of Mat_2 of the sensitivity study.

Thickness	LPF	P_c
10	0,51374	30,82440
20	0,51856	31,11402
30	0,52861	31,71690
40	0,54306	32,58378
50	0,56167	33,70038
60	0,58492	35,09562
70	0,61303	36,78192
80	0,64651	38,79078
90	0,68266	40,96014
100	0,72013	43,20822
110	0,75773	45,46416
120	0,79774	47,86440

TABLE B.5: Results of Mat_3 of the sensitivity study.

Thickness	LPF	P_c
10	0,51374	30,82440
20	0,51857	31,11402
30	0,52862	31,71690
40	0,54306	32,58378
50	0,56167	33,70038
60	0,58493	35,09562
70	0,61316	36,78948
80	0,64652	38,79090
90	0,68273	40,96386
100	0,72029	43,21734
110	0,75844	45,50640
120	0,79866	47,91984

TABLE B.6: Results of Mat_4 of the sensitivity study.

Thickness	LPF	P_c
10	0,51374	30,82440
20	0,51857	31,11402
30	0,52862	31,71690
40	0,54306	32,58378
50	0,56167	33,70038
60	0,58493	35,09562
70	0,61303	36,78192
80	0,64652	38,79096
90	0,68242	40,94532
100	0,71978	43,18650
110	0,75803	45,48204
120	0,79816	47,88984

TABLE B.7: Results of *PP-PNM* of the sensitivity study.

Thickness	LPF	P_c
10	0,51203	30,7219
20	0,51420	30,8521
30	0,51927	31,1562
40	0,52778	31,6666
50	0,53948	32,3687
60	0,55316	33,1898
70	0,56957	34,1743
80	0,58773	35,2640
90	0,60743	36,4455
100	0,62742	37,6450
110	0,64845	38,9071
120	0,66941	40,1646

TABLE B.8: Results of *PP-ISO* of the sensitivity study.

Thickness	LPF	P_c
10	0,51374	30,8244
20	0,51857	31,1140
30	0,52862	31,7169
40	0,54306	32,5838
50	0,56167	33,7004
60	0,58433	35,0599
70	0,60950	36,5699
80	0,63573	38,1439
90	0,66269	39,7613
100	0,69119	41,4713
110	0,72081	43,2485
120	0,75277	45,1662

TABLE B.9: Results of *PP-FOAM* of the sensitivity study.

Thickness	LPF	P_c
10	0,51181	30,70884
20	0,51334	30,80034
30	0,51761	31,05660
40	0,52448	31,46862
50	0,53397	32,03844
60	0,54551	32,73042
70	0,55892	33,53532
80	0,57325	34,39482
90	0,58826	35,29542
100	0,60472	36,28290
110	0,62114	37,26834
120	0,63869	38,32164

B.4 Results of Case study.

Collapse pressures follows:

P_c = ABAQUS coated pipe

P_0 = ABAQUS uncoated pipe

P_1 = Haagsma (DNV) equation (uncoated pipe)

TABLE B.10: Result of case study for material with elasticity of 250 MPa for coating ovality of 0.5%.

Thickness	LPF	P_c	$\frac{P_c}{P_0}$	$\frac{P_c}{P_1}$
0	0,513123	30,78738	1	0,950521
10	0,512617	30,75702	0,999013	0,949583
20	0,512461	30,74766	0,998709	0,949294
30	0,51276	30,76560	0,999292	0,949848
40	0,51362	30,81720	1,000968	0,951441
50	0,514888	30,89328	1,003439	0,953790
60	0,517529	31,05174	1,008586	0,958682
70	0,519584	31,17504	1,012591	0,962489
80	0,521552	31,29312	1,016426	0,966135
90	0,525306	31,51836	1,023742	0,973089
100	0,529524	31,77144	1,031963	0,980902
110	0,53353	32,01180	1,039770	0,988323
120	0,534489	32,06934	1,041639	0,990100

TABLE B.11: Result of case study for material with elasticity of 500 MPa for coating ovality of 0.5%.

Thickness	LPF	P_c	$\frac{P_c}{P_0}$	$\frac{P_c}{P_1}$
0	0,513123	30,78738	1	0,951990
10	0,511518	30,69108	0,996872	0,949012
20	0,511148	30,66888	0,996151	0,948326
30	0,512422	30,74532	0,998633	0,950690

TABLE B.11: *Continued*

40	0,514663	30,87978	1,003001	0,954847
50	0,518048	31,08288	1,009598	0,961128
60	0,522367	31,34202	1,018015	0,969141
70	0,528572	31,71432	1,030107	0,980653
80	0,535334	32,12004	1,043285	0,993198
90	0,542548	32,55288	1,057344	1,006582
100	0,54899	32,9394	1,069899	1,018534
110	0,556928	33,41568	1,085369	1,033261
120	0,566205	33,9723	1,103448	1,050473

TABLE B.12: Result of case study for material with elasticity of 750 MPa for coating ovality of 0.5%.

Thickness	LPF	P_c	$\frac{P_c}{P_0}$	$\frac{P_c}{P_1}$
0	0,513123	30,78738	1	0,951990
10	0,510553	30,63318	0,994991	0,947222
20	0,510605	30,63630	0,995092	0,947319
30	0,512243	30,73458	0,998285	0,950358
40	0,515855	30,95130	1,005324	0,957059
50	0,521124	31,26744	1,015592	0,966834
60	0,528799	31,72794	1,030550	0,981074
70	0,537658	32,25948	1,047815	0,997510
80	0,547749	32,86494	1,067480	1,016231
90	0,558369	33,50214	1,088177	1,035935
100	0,569547	34,17282	1,109961	1,056673
110	0,582137	34,92822	1,134497	1,080031
120	0,594175	35,65050	1,157958	1,102365

TABLE B.13: Result of case study for material with elasticity of 1000 MPa for coating ovality of 0.5%.

Thickness	LPF	P_c	$\frac{P_c}{P_0}$	$\frac{P_c}{P_1}$
0	0,513123	30,78738	1	0,951990

TABLE B.13: *Continued*

10	0,509622	30,57732	0,993177	0,945495
20	0,510459	30,62754	0,994808	0,947048
30	0,515194	30,91164	1,004036	0,955833
40	0,522179	31,33074	1,017648	0,968792
50	0,532405	31,9443	1,037577	0,987764
60	0,543897	32,63382	1,059973	1,009085
70	0,557758	33,46548	1,086986	1,034801
80	0,572394	34,34364	1,115510	1,061955
90	0,587668	35,26008	1,145277	1,090293
100	0,604447	36,26682	1,177976	1,121423
110	0,621729	37,30374	1,211656	1,153486
120	0,638813	38,32878	1,244951	1,185181

TABLE B.14: Result of case study for material with elasticity of 250 MPa for coating ovality of 1.0%

Thickness	LPF	P_c	$\frac{P_c}{P_0}$	$\frac{P_c}{P_1}$
0	0,513123	30,78738	1	0,950521
10	0,512771	30,76626	0,999314	0,949869
20	0,512756	30,76536	0,999284	0,949841
30	0,513138	30,78828	1,000029	0,950548
40	0,514048	30,84288	1,001802	0,952234
50	0,515324	30,91944	1,004289	0,954598
60	0,517872	31,07232	1,009255	0,959318
70	0,51996	31,1976	1,013324	0,963186
80	0,521929	31,31574	1,017161	0,966833
90	0,525645	31,5387	1,024403	0,973717
100	0,529774	31,78644	1,032450	0,981365
110	0,533746	32,02476	1,040191	0,988723
120	0,53475	32,085	1,042147	0,990583

TABLE B.15: Result of case study for material with elasticity of 500 MPa for coating ovality of 1.0%

Thickness	LPF	P_c	$\frac{P_c}{P_0}$	$\frac{P_c}{P_1}$
0	0,513123	30,78738	1	0,950521
10	0,512311	30,73866	0,998417	0,949016
20	0,512211	30,73266	0,998222	0,948831
30	0,513479	30,80874	1,000693	0,951180
40	0,515771	30,94626	1,005160	0,955426
50	0,51912	31,1472	1,011687	0,961630
60	0,523384	31,40304	1,019997	0,969528
70	0,529501	31,77006	1,031918	0,980860
80	0,536106	32,16636	1,044790	0,993095
90	0,543131	32,58786	1,058481	1,006108
100	0,549565	32,9739	1,071020	1,018027
110	0,557386	33,44316	1,086261	1,032514
120	0,565257	33,91542	1,101601	1,047095

TABLE B.16: Result of case study for material with elasticity of 750 MPa for coating ovality of 1.0%

Thickness	LPF	P_c	$\frac{P_c}{P_0}$	$\frac{P_c}{P_1}$
0	0,513123	30,78738	1	0,950521
10	0,511927	30,71562	0,997669	0,948305
20	0,512173	30,73038	0,998148	0,948761
30	0,513933	30,83598	1,001578	0,952021
40	0,517555	31,0533	1,008637	0,958731
50	0,52277	31,3662	1,018800	0,968391
60	0,530234	31,81404	1,033346	0,982217
70	0,538835	32,3301	1,050108	0,998150
80	0,548697	32,92182	1,069328	1,016419
90	0,559111	33,54666	1,089623	1,035710
100	0,570085	34,2051	1,111010	1,056038
110	0,582419	34,94514	1,135047	1,078886
120	0,594331	35,65986	1,158262	1,100952

TABLE B.17: Result of case study for material with elasticity of 1000 MPa for coating ovality of 1.0%

Thickness	LPF	P_c	$\frac{P_c}{P_0}$	$\frac{P_c}{P_1}$
0	0,513123	30,78738	1	0,950521
10	0,511814	30,70884	0,997448	0,948096
20	0,513339	30,80034	1,000420	0,950921
30	0,51761	31,0566	1,008744	0,958832
40	0,524477	31,46862	1,022127	0,971553
50	0,533974	32,03844	1,040635	0,989146
60	0,545507	32,73042	1,063111	1,010510
70	0,558922	33,53532	1,089255	1,035360
80	0,573247	34,39482	1,117172	1,061896
90	0,588257	35,29542	1,146424	1,089701
100	0,604715	36,2829	1,178499	1,120188
110	0,621139	37,26834	1,210507	1,150612
120	0,638694	38,32164	1,244719	1,183131

TABLE B.18: Result of case study for material with elasticity of 250 MPa for coating ovality of 1.5%

Thickness	LPF	P_c	$\frac{P_c}{P_0}$	$\frac{P_c}{P_1}$
0	0,513123	30,78738	1	0,950521
10	0,51287	30,7722	0,999506	0,950052
20	0,513052	30,78312	0,999861	0,950389
30	0,513578	30,81468	1,000886	0,951364
40	0,5146	30,876	1,002878	0,953257
50	0,515945	30,9567	1,005499	0,955748
60	0,518435	31,1061	1,010352	0,960361
70	0,520615	31,2369	1,014600	0,964399
80	0,522637	31,35822	1,018541	0,968145
90	0,526318	31,57908	1,025715	0,974963

<div style="text-align: center;">TABLE B.18: Continued</div>

100	0,530317	31,81902	1,033508	0,982371
110	0,534229	32,05374	1,041132	0,989618
120	0,535369	32,12214	1,043354	0,991730

TABLE B.19: Result of case study for material with elasticity of 500 MPa for coating ovality of 1.5%

Thickness	LPF	P_c	$\frac{P_c}{P_0}$	$\frac{P_c}{P_1}$
0	0,513123	30,78738	1	0,950521
10	0,51306	30,7836	0,999877	0,950404
20	0,513505	30,8103	1,000744	0,951228
30	0,514811	30,88866	1,003289	0,953648
40	0,51727	31,0362	1,008081	0,958203
50	0,520714	31,24284	1,014793	0,964582
60	0,525031	31,50186	1,023206	0,972579
70	0,5311	31,866	1,035034	0,983822
80	0,536642	32,19852	1,045835	0,994088
90	0,543528	32,61168	1,059254	1,006844
100	0,550827	33,04962	1,073479	1,020364
110	0,558402	33,50412	1,088242	1,034397
120	0,566156	33,96936	1,103353	1,048760

TABLE B.20: Result of case study for material with elasticity of 750 MPa for coating ovality of 1.5%

Thickness	LPF	P_c	$\frac{P_c}{P_0}$	$\frac{P_c}{P_1}$
0	0,513123	30,78738	1	0,950521
10	0,513272	30,79632	1,000290	0,950797
20	0,513979	30,83874	1,001668	0,952106
30	0,516083	30,96498	1,005768	0,956004
40	0,519913	31,19478	1,013232	0,963099
50	0,525224	31,51344	1,023583	0,972937
60	0,532641	31,95846	1,038037	0,986676

TABLE B.20: *Continued*

70	0,540976	32,45856	1,054281	1,002116
80	0,550521	33,03126	1,072883	1,019798
90	0,560652	33,63912	1,092626	1,038564
100	0,571321	34,27926	1,113419	1,058328
110	0,582491	34,94946	1,135187	1,079020
120	0,594822	35,68932	1,159219	1,101862

TABLE B.21: Result of case study for material with elasticity of 1000 MPa for coating ovality of 1.5%

Thickness	LPF	P_c	$\frac{P_c}{P_0}$	$\frac{P_c}{P_1}$
0	0,513123	30,78738	1	0,950521
10	0,51407	30,8442	1,001845	0,952275
20	0,516123	30,96738	1,005846	0,956078
30	0,520716	31,24296	1,014797	0,964586
40	0,527771	31,66626	1,028546	0,977655
50	0,53711	32,2266	1,046747	0,994955
60	0,54822	32,8932	1,068398	1,015535
70	0,56078	33,6468	1,092876	1,038802
80	0,574947	34,49682	1,120485	1,065045
90	0,589558	35,37348	1,148960	1,092111
100	0,605432	36,32592	1,179896	1,121516
110	0,621478	37,28868	1,211167	1,151240
120	0,63855	38,313	1,244438	1,182865

TABLE B.22: Results of serial resistance collapse capacity.

Thickness	LPF	P_c	$\frac{P_c}{P_0}$	$\frac{P_c}{P_1}$
10	0,016678495	30,7966785	1,000541861	
20	0,117472827	30,89747283	1,003816531	
30	0,35023167	31,13023167	1,011378547	
40	0,734955516	31,51495552	1,023877697	

TABLE B.22: *Continued*

50	1,265355508	32,04535551	1,041109666
60	1,903566841	32,68356684	1,061844277
70	2,555131705	33,33513171	1,083012726
80	3,114847977	33,89484798	1,10119714
90	3,565886259	34,34588626	1,115850756
100	3,95159607	34,73159607	1,128381939
110	4,294394156	35,07439416	1,139518978
120	4,604094735	35,38409474	1,149580726